Investigation of Power Harvesting Potential from Vehicle Suspension Systems

by

Farhang Jalilian
B.Sc. Electrical Engineering, K.N.Toosi University of Technology, 2011

A Thesis Submitted in Partial Fulfillment
of the Requirements for the Degree of

MASTER OF APPLIED SCIENCE

in the Department of Electrical and Computer Engineering

Supervisory Committee

Investigation of Power Harvesting Potential from Vehicle Suspension Systems

by

Farhang Jalilian
B.Sc. K.N.Toosi University of Technology, 2011

Supervisory Committee

Dr. Amirali Baniasadi (Department of Electrical and Computer Engineering)
Supervisor

Dr. Hong-Chuan Yang (Department of Electrical and Computer Engineering)
Departmental Member

Dr. Brad Buckham (Department of Mechanical Engineering)
Outside Member

Abstract

Supervisory Committee
Dr. Amirali Baniasadi (Department of Electrical and Computer Engineering)
Supervisor

Dr. Hong-Chuan Yang (Department of Electrical and Computer Engineering)
Departmental Member

Dr. Brad Buckham (Department of Mechanical Engineering)
Outside Member

This thesis revisits the concept of ground vehicles active suspensions system from a power harvesting perspective. I introduce the *two dimensions of freedom quarter* vehicle model for calculations of vehicle dynamics as well as a road profile model based on PSD classifications based on International Organization for Standardization's technical document, ISO 8608 "Mechanical vibration -- Road surface profiles -- Reporting of measured data". I report the power harvesting potential of the conventional viscous fluid dampers for an extensive range of road profile roughness indices and vehicle speeds. I explain the problem of additional power harvesting from the regenerative electric damper operating in the "dead-zone" and introduce Pulse Width Modulated (PWM) DC-DC converter as a solution. I analyze the efficiency of this system by circuit level simulations in PSpice.

Table of Contents

List of Tables

List of Figures

Acknowledgements

I would like to express my deepest gratitude to my supervisor Dr. Amirali Baniasadi for believing in me and for his guidance, patience and support through every stage this research. Besides the technical knowledge, I learnt so many invaluable lessons about life from him. I feel very lucky that I was given the chance to work under his supervision.

I would like to extend my sincerest thanks and appreciation to Dr. Nikitas Dimopoulos for his advice on my research. Many thanks to Dr. Mihai Sima, Dr. Wu-Sheng Lu, and Dr. Daler N.Rakhmatov who built my technical background and provided me with advanced knowledge in different fields of engineering.

I would also like to thank the staff at University of Victoria, Janice Closson, Moneca Bracken who eased my path through graduation process. Also many thanks to Kevin Jones and Steve Campbell for their technical support.

Despite being away from home, my family in Toronto and my best friends in Victoria made every day of my journey with best memories. I would like to thank Khale Zohre, Amu Behruz, Mehdi and Amir for being there for me whenever I needed them. Navid, Ali, Ebad and Mohammad thank you all who are always in my heart.

Dedication

To my beloved parents Marzieh and Hamid, and my brother Farhad for their never ending and immeasurable love and support.

Chapter 1

Introduction

Transportation is an essential societal need in the current era. The increases in population and economic growth have created higher demand for transportation. The worldwide number of cars currently is approximately 1 billion and is expected to increase to 1.7 billion by 2035 [1].

Undoubtedly transportation is one of the major factors in the worldwide energy consumption today. According to the Transport Energy and CO_2 report by The International Energy Agency (IEA) transportation accounts for 19% of total energy usage globally and 23% of total energy related carbon monoxide emissions. The latter is expected to increase approximately 50% by 2030 and more than 80% by 2050 [2].

The Intergovernmental Panel on Climate Change (IPCC) suggests a reduction of at least 50% in CO_2 emissions by 2050 in order to avoid the effects of huge climate change. As mentioned above, transportation is a non-negotiable part of this goal. Without cuts in CO_2 emissions in the transportation sector, it would be very difficult to achieve targets such as stabilising the concentration of greenhouse gas (GHG) emissions in the atmosphere at a level of 450 ppm of CO_2 equivalent [3].

1.1. Motor vehicle efficiency and performance indices

Improving efficiency of vehicles, by improving fuel economy translates directly to reducing the CO_2 emissions. Unfortunately conventional vehicles that use internal combustion engine (ICE) waste most of the energy stored in the fuel hence are known for their low efficiency. According to the U.S Department of Energy's office of

transportation and air quality only about 14% to 26% of the energy released from the combustion of the fuel is used to propel the cars, depending on the "drive cycle"[1] [4].

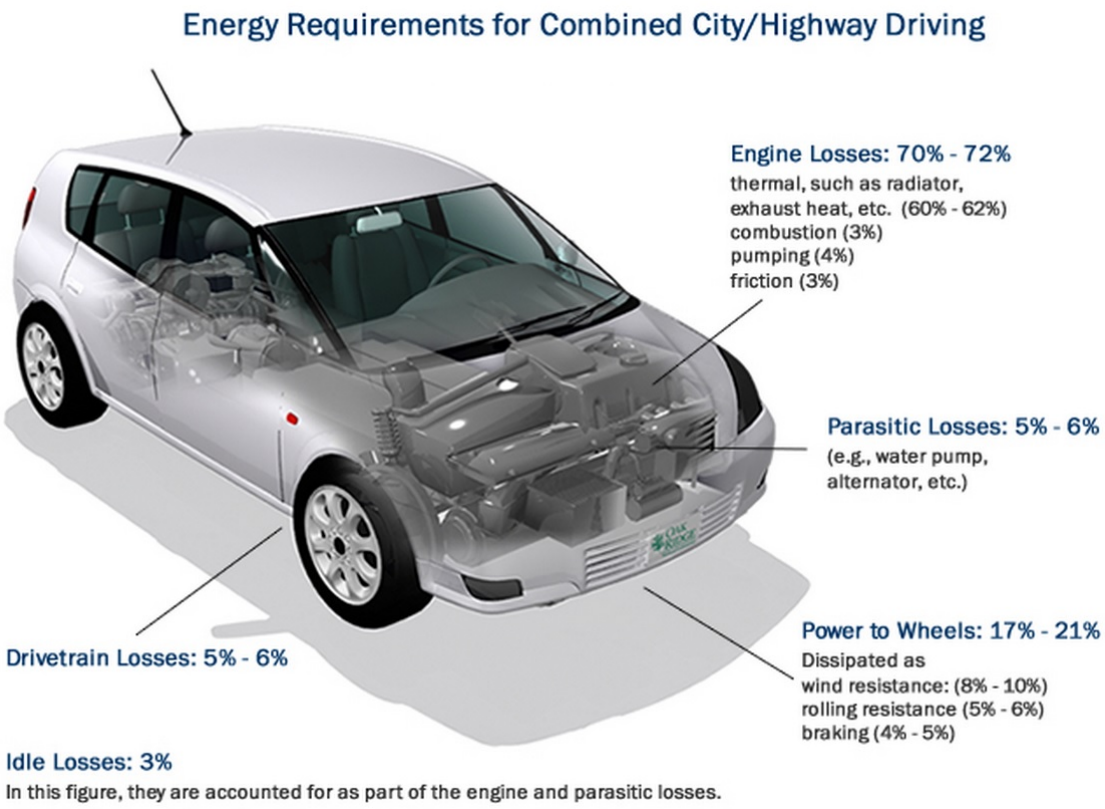

Figure 1-1 Where energy goes in Internal Combustion Engine (ICE) vehicles taken from [4]

The biggest individual energy waste is waste heat in ICEs. Thermal losses, such as the loss of energy in the radiator and the heat loss from the exhaust, in total accounts for 60 to 62% of the whole energy waste. Other forms of energy loss include losses due to wind resistance (8 to 10%), rolling resistance (5 to 6%), braking (4 to 5%), parasitic (5 to 6%), drive train losses (5 to 6%) and idle losses (3%). These numbers relate to combined driving mode in city and highway [4].

Redesigning and applying new technologies to each of the components of a vehicle, which are subject to power loss in different forms, can lead to better overall performance

[1] A drive cycle test is aimed to measure the speed of the vehicle in time domain for different drive conditions.

and improvements in fuel economy of the vehicle. Aside from significant cost savings for the users, these technologies contribute to the goal of saving the environment by reducing GHG emissions which is the door to many other benefits for all human beings and animals.

A feasible example of such technology is the *regenerative braking system* (or "regen" in short). A regenerative braking system is designed to recover the kinetic energy that is lost during braking. Imagine a car cruising at the speed of V_0, the driver pushes the brake and reduces the speed to $V_1 < V_0$. In this simple event, disregarding all other losses, a total energy of $E = \frac{1}{2}m(V_1 - V_0)^2$ should be taken from the system. According to the first law of thermodynamics, the energy in a system is not created or destroyed, but changes form. In the case of braking, the energy is not lost, but changes from kinetic form to the form of heat in the brake discs. Regenerative braking technology recovers this energy into a useful form, such as kinetic energy in a flywheel or chemical energy in the battery, so that it can be utilized later. The latter is more feasible in electric vehicles (EV) or hybrids (HEV) in which the stored energy in the battery is the main source of energy available. Also regenerative braking is easier to implement in EVs or HEVs since electric motors are already mechanically coupled to the power train system. Hence instant switching between accelerating/decelerating (braking) modes is possible using a smart control system. The regenerative braking is already implemented in most current EV and HEVs available today. However regenerative suspension is a relatively new concept and research in this area has been very popular in the last three decades.

1.2. Research motivations

This thesis focuses on the energy losses that happen in the suspension system of vehicles. The suspension system of a vehicle is an essential component that is designed to suppress the effect of mechanical vibrations of wheels, caused naturally by driving on road undulations, to the chassis and passengers. The damper of most conventional suspension systems is a viscous damper, composed of a piston and a viscous fluid inside the piston. The damper works by dissipating the input kinetic energy of the force applied to it into the hydraulic fluid in the form of heat, hence the alternative name of shock absorber.

With newer technologies such as electric active suspensions, harvesting power from the suspension system is achievable. The main motivation of this thesis to characterise the power harvesting potential in such advanced suspensions. This thesis assumes that power harvesting potential in active and semi-active suspensions belong to their damping properties, similar to a conventional suspension. This thesis is aimed at finding the power losses in a conventional suspension and suggests that the same power can be harvested in an active suspension in regenerative mode.

1.3. Thesis outline

In Chapter 2, I introduce the two dimension of freedom (2-DOF) quarter car vehicle model along with its governing equations of motion and use MATLAB Simulink for the goal of estimating the power harvesting potential in a suspension system of a vehicle for a given input road profile.

In Chapter 3, I explain the problem of road modelling the approach to simulating a random road profile based on standard classes of roads [5]. Chapter 4 is dedicated to the

results of the simulation for a set of road roughness indices each calculated at different vehicle speeds.

Chapter 5 is dedicated to introducing the electrical power aspects of the active damper and storage devices in conventional and modern vehicles. I outline the problem of dead zone operation of active suspensions and introduce PWM DC-DC converters as a solution.

Chapter 6 summarizes conclusions and contributions. It ends this thesis with the research motivations for the future.

Chapter 2

Vehicle Suspension Systems

Suspension systems are deployed in most mechanical systems in order to smoothen the mechanical movements and vibrations that affect those systems. In vehicles, the chassis (body) of the vehicle is subject to vibrations which are due to several factors such as the road irregularities (e.g. potholes), aerodynamic forces and engine and transmission vibrations. A possible categorization of these vibration forces can be derived by determining the point of application of each of these forces. Vibration forces from road irregularities are applied to the vehicle body and passengers through the suspension system while aerodynamic forces and engine vibrations are applied directly to the vehicle body [6].

The suspension systems play an important role of providing comfort for the passengers as well as protecting the engine and other mechanical parts of the vehicle from harsh vibrations that are otherwise induced by road roughness.

2.1. Passive suspension systems

A conventional suspension system used in most passenger cars is consisted of a mechanical spring and a damper connected in parallel, hence the name passive. Figure 2 shows the McPherson suspension system which is the most common suspension used in current vehicles. It is a strut-type suspension basically composed of a damper and spring connected in parallel [7].

The damper damps the unwanted vertical vibrations caused by road undulations and the spring keeps the wheel in contact with road.

Figure 2-1 McPherson suspension system

Photo credit Christopher J Longhurst [7]

Ride comfort and handling are two important measures of quality of a vehicle. These two factors depend on how each part of the vehicle is designed. One of the components that plays an important role in ride comfort and handling of a car is the suspension system. Conventional passive suspensions, from the physics point of view, basically have two design parameters, spring's stiffness (k) and damper's coefficient (c).

A general rule of thumb considered in choosing these two parameters is that the stiffer and shorter the suspension system is, the better ride handling and the worse the ride comfort is and vice versa. This natural trade-off forms the biggest limitation of conventional passive suspensions systems. Hence the designer of a suspension system has to decide an optimum value of k and c which work best for the each individual vehicle and suitable for its general purpose. For example luxury cars suspension would be

optimized for ride comfort compared to race cars' which would be optimized for ride handling.

After the characteristics of the passive suspension system is chosen and the suspension design is finalized and the suspension is mass-produced, the values c and k are fixed and cannot be changed after production.

2.2. Advanced vehicle suspension systems

During the last three decades automotive researchers have proposed and designed new types of suspensions in order to overcome the limitations of conventional passive suspension. The name *Active suspension* is given to this new generation of dampers since they are composed of active elements which can consume power and generate dynamically controlled response (force) in real time. The generated force by active suspensions is fully controllable and thus the suspension system is capable of switching between states with different mechanical characteristics according to the controller command. The controller itself senses the environmental variables such as the road roughness, cruising speed and the driver's commands. These inputs are then combined in the controller which dynamically controls the force generated by each active suspension using a complex algorithm.

Several studies have been conducted in the field of active suspensions in an effort to make them more feasible to be used in low cost cars and to improve their power consumption. The main challenges associated with active suspension are its power consumption, reliability and production cost [8].

To overcome the problems aligned with active suspension, researchers have come up with *semi-active suspension* which is proposed to benefit from the advantages of passive

and active suspension. Semi-active suspensions are more reliable compared to active suspensions since they use a fail-safe passive damper or spring in parallel to the active part. Also they are less power hungry as a portion of required suspension force is generated by the passive part. However they are fundamentally less tunable compared to a fully-active suspension system.

This thesis assumes a passenger car with conventional passive suspension. The main interest of this thesis is to explore the potential of power harvesting in a suspension system using an energy converter. This converter can be mechanical (e.g. flywheel) or electrical (e.g. linear motor/generator). It is important to the goal of power harvesting to have a model of the power loss in the damper before designing the converter. Hence most of this thesis is dedicated to feasibility studies aimed at characterising the power harvesting potential in the damper of passenger car suspension system.

In order to model the power dissipation in a passenger vehicle's suspension system, there’s a need to model the dynamics of the car and the road discussed in chapter 2 and 3 respectively.

2.3. Two Dimension of Freedom (2-DOF) quarter-car vehicle model

For the purpose of simulating vehicle dynamics, this thesis considers a two dimension of freedom (2-DOF) quarter-car vehicle model. Quarter-car model means that the simulation model is going to include only one wheel of the vehicle. This model only assumes upward/downward movements for the two masses, hence the name.

The 2-DOF quarter vehicle model is shown in Fig. 2-2. It is composed of a sprung mass (mass of the body) and an unsprung mass, defined as mass of one wheel, the axis and everything that is connected to the wheel. The damper and the spring of the

suspension system are modeled as C_1 and K_1 respectively. The equivalent spring of the tire is assumed as K_2. The small damping effect of the tire is neglected (i.e. C_2=0).

The free body diagram of the 2-DOF quarter car model is sketched in Figure 2-2. We will use the force applied to each element in order to derive the equations of motion.

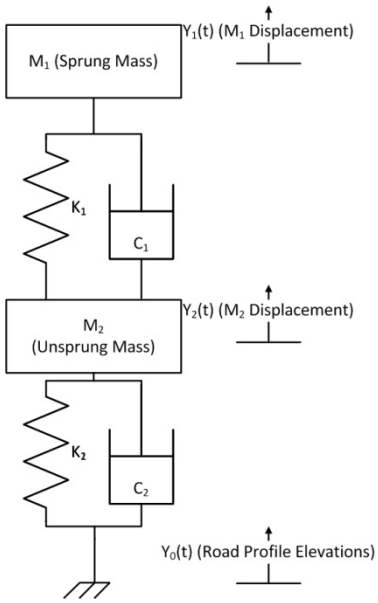

Figure 2-2 Two Dimension of Freedom (2-DOF) quarter car model

The system of differential equations that govern the motion of masses in the 2-DOF quarter car are as follows:

$$m_1\ddot{y}_1 + c_1(\dot{y}_1 - \dot{y}_2) + k_1(y_1 - y_2) = 0 \quad \textbf{(2-1)}$$

$$m_2\ddot{y}_2 + c_1(\dot{y}_2 - \dot{y}_1) + k_1(y_2 - y_1) + c_2\dot{y}_2 + k_2y_2 = c_2\dot{y}_0 + k_2y_0 \quad \textbf{(2-2)}$$

I use the equations above to simulate the dynamics of vehicle in response to road profile undulations. I solved the equations using both numerical methods, ode45 numerical solver of MATLAB for differential equations, and also using Simulink which is a block diagram environment for model-based design. The results of the hardcoded

ode45 solution lined up with the Simulink outputs; hence the Simulink model was used exclusively for the rest of the work.

2.4. Power dissipation in viscous damper

The power dissipation in a viscous damper having damping coefficient *c* and connected between two masses with displacements y_1 (from and y_{1a} to y_{1b}) and y2 (from and y_{2a} to y_{2b}) is calculated as follows [9].

$$W = \int_{y_{1a}}^{y_{1b}} c(\dot{y}_2 - \dot{y}_1)dy_1 - \int_{y_{2a}}^{y_{2b}} c(\dot{y}_2 - \dot{y}_1)dy_2 \quad \textbf{(2-3)}$$

$$P = -\frac{dW}{dt} \quad \textbf{(2-4)}$$

$$dy = \dot{y}\, dt \quad \textbf{(2-5)}$$

$$P = -\frac{d}{dt}\left[\int_{y_{1a}}^{y_{1b}} c(\dot{y}_2 - \dot{y}_1)dy_1 - \int_{y_{2a}}^{y_{2b}} c(\dot{y}_2 - \dot{y}_1)dy_2\right] \quad \textbf{(2-6)}$$

$$= -\frac{d}{dt}\left[\int_{t_1}^{t_2} c(\dot{y}_2 - \dot{y}_1)\dot{y}_1 dt\right] + \frac{d}{dt}\left[\int_{t_1}^{t_2} c(\dot{y}_2 - \dot{y}_1)\dot{y}_2 dt\right] \quad \textbf{(2-7)}$$

$$= c(\dot{y}_2 - \dot{y}_1)^2 \quad \textbf{(2-8)}$$

2.5. Simulink model of the 2-DOF quarter car model

The following is a diagram of the Simulink model of the 2-DOF quarter car model. The road profile input is fed into this Simulink model. The output of this simulation is sampled data of the motions (as well as velocity and acceleration) of sprung and unsprung masses and the power generated as a result of damper expansion and compression.

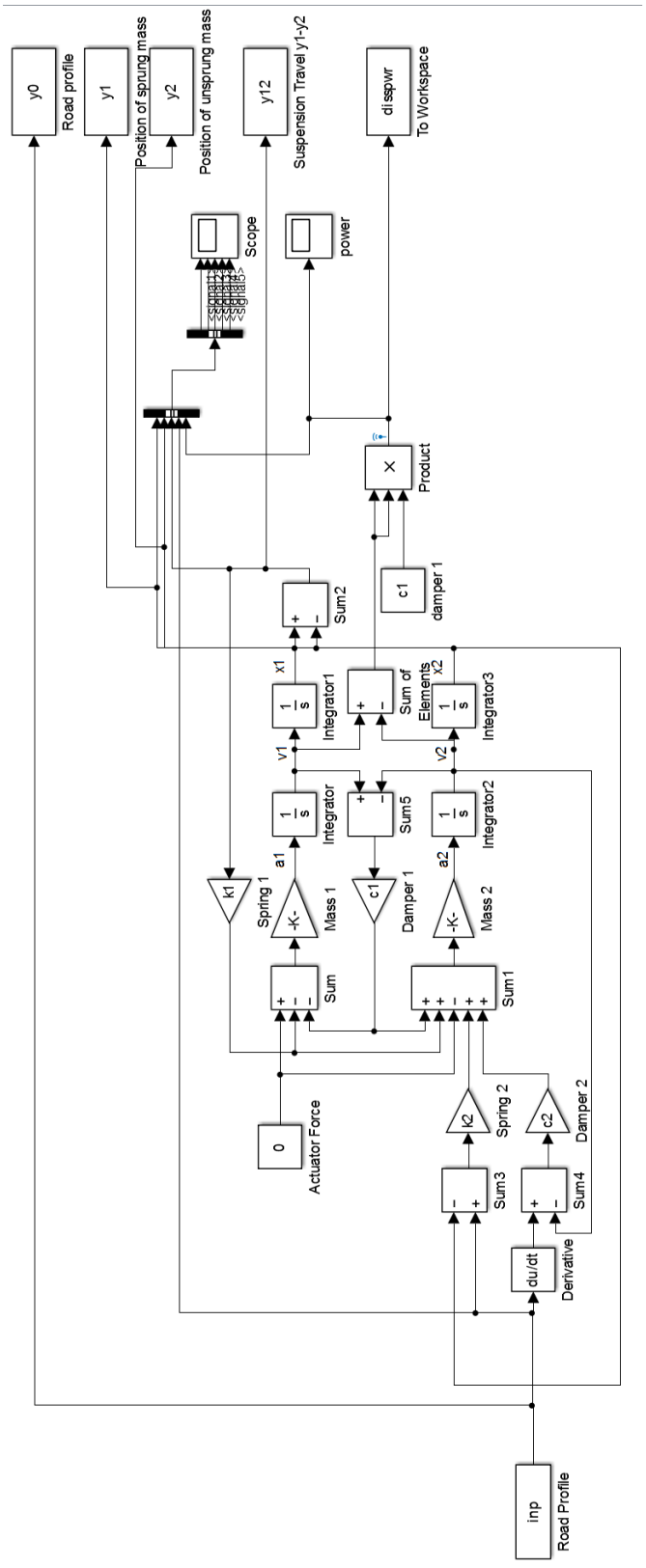

Figure 2-3 The block diagram of the 2-DOF car model designed in Simulink

2.6. Frequency response of the 2-DOF car model

The equations of force and motion mentioned in the last part are sufficient for explaining the vehicle dynamics, i.e. movements of masses and travel of the spring and dampers. However to gain more insight into the model, we need to analyse the system in frequency domain. I have analytically derived the transfer function of both system outputs $Y_1(s)$ and $Y_2(s)$ as follows, neglecting the small damping coefficient of the tire, i.e $C_2 = 0$:

$$\frac{Y_1(s)}{Y_0(s)} = \frac{s(c_1k_2) + k_1k_2}{s^4(m_1m_2) + s^3\big(c_1(m_1+m_2)\big) + s^2(k_1(m_1+m_2) + k_2m_1) + s(c_1k_2) + k_1k_2} \quad \textbf{(2-9)}$$

$$\frac{Y_2(s)}{Y_0(s)} = \frac{s^2(m_1k_2) + s(c_1k_2) + k_1k_2}{s^4(m_1m_2) + s^3\big(c_1(m_1+m_2)\big) + s^2(k_1(m_1+m_2) + k_2m_1) + s(c_1k_2) + k_1k_2} \quad \textbf{(2-10)}$$

$$\frac{Y_1(s) - Y_2(s)}{Y_0(s)} = \frac{-s^2(m_1k_2)}{s^4(m_1m_2) + s^3\big(c_1(m_1+m_2)\big) + s^2(k_1(m_1+m_2) + k_2m_1) + s(c_1k_2) + k_1k_2} \quad \textbf{(2-11)}$$

In order to plot these functions in frequency (Hz) domain, the following conversion is made:

$$s = jw = j * 2\pi f \qquad \textbf{(2-12)}$$

The parameters of the vehicle and its suspension are presented in Table 4.1.

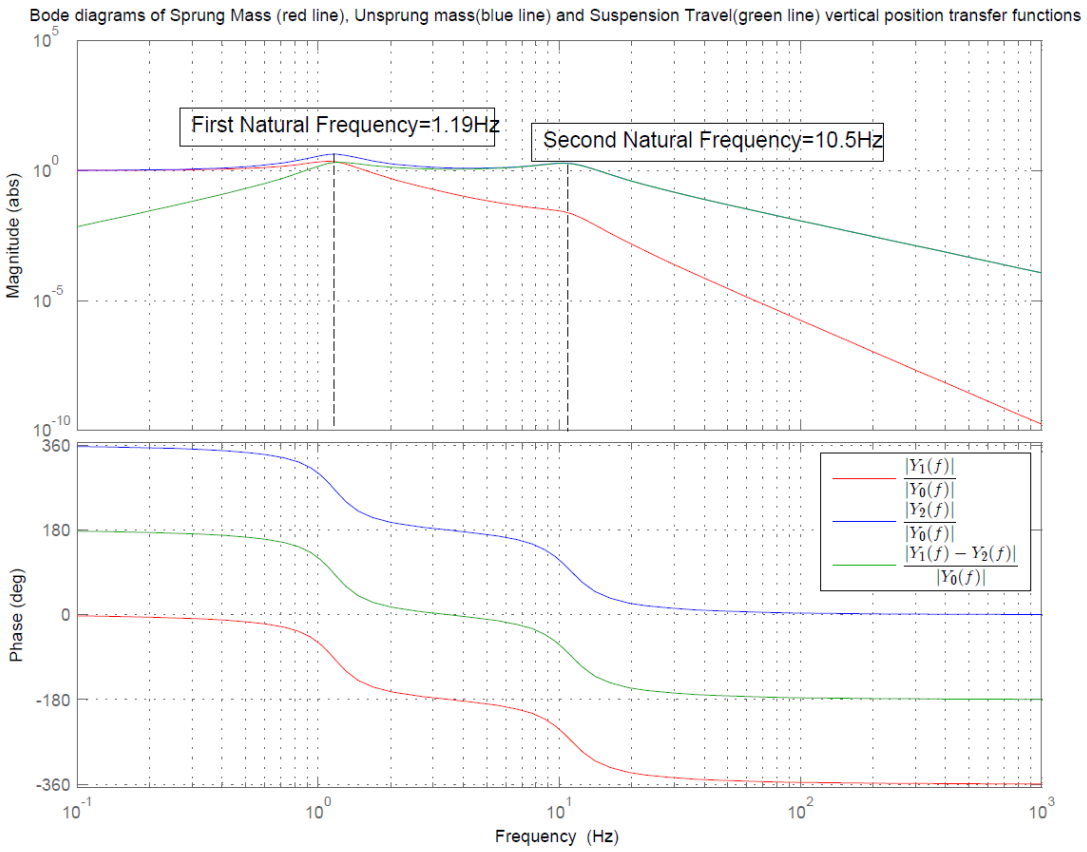

Figure 2-4 Bode diagrams of Sprung Mass (red line), Unsprung Mass (blue line) and Suspension Travel's (green line) vertical position transfer functions

As the bode plot of the Eq. 2-9 (red line) in Fig 2-4 shows, the conventional suspension system is designed to damp road undulations from frequencies of 1.19 Hz and above to provide comfort for the passengers. This is performed by the change in suspension length or suspension travel. As the bode plot of Eq. 2-11 in Fig 2-4 (blue line) shows, the travel of the suspension absorbs most undulations of the road profile, and at natural frequencies it even amplifies the input.

Chapter 3

Road Modelling

A motor vehicle like any other mechanical system is subject to several sources of vibration, either from internal or external sources. Engine vibration, due to movement of its different mechanical components, is one of the major internal sources of vibration. On the other hand vibrations induced to the body of the vehicle from the wheels traversing on road undulations is the main source of external vibrations.

While automotive engineers have some control over the internal sources of vibration, this is not the case regarding external ones. Having a model describing the behavior and characteristics of external sources of vibration is important to engineers and designers since less information is known on their behavior compared to internal parts [6]. Many researchers have tackled the problem of road modelling road profile, an extensive list of these publications can be found at [8].

This chapter of the thesis addresses the modelling the road profile a typical passenger car might travel on. This includes a wide range of roads with different roughness degrees from highways as a good quality road with minimal irregularities to very poor quality off-road tracks with potholes and stones. Having the road profile and a vehicle model, I aim to simulate the dynamics of the vehicle and report and analyze dynamics of the system of interest e.g. displacement, acceleration or stress at each component both in time and frequency domain.

3.1. Direct measurement of road profiles

The Motor Industry Research Association (MIRA) ran a survey of measurement of different types of roads in Britain, France, Belgium and Western Germany [6]. The following is a summary of their approach to measuring the road profiles.

There are several issues with measuring the road profile directly by reading elevations from a reference point. One of the significant problems is that the measurement device should be isolated from the road undulations. Hence a datum needs to be set up as a reference point. The datum has to be long enough to be able to cover long wavelengths. The datum length has to be at least double the longest wavelength of interest in the measurement of road irregularities. R.P La Barre *et al* bound the frequencies of interest (for structural and riding considerations) from 0.5 to 50 Hz [6]. Assuming the vehicle spends most of the time traveling at the speeds between 20 to 100 mph (32.2 Km/h to 160.9 Km/h), the range of wavelengths of interest will be 0.6 ft. to 300 ft. (0.18 to 19.1 meters). Hence the length of the datum, which has to be longer than (at least twice) the maximum wavelength of interest, is one issue. Several alternatives to be used as a datum were assumed, such as a simple mechanical edge, a light beam and a mechanical averaging method that finds the average height of the road. Another method is measuring the slope and calculating the displacement from this [6].

The MIRA report explains the details of the measurement of road profile a passenger car is subject to, using analog electronic devices. R.P La Barre *et al* measured the variations from the road surface to a reference point in a vehicle and the variations in distance from the road surface to the reference point, separately. The measurement system is composed of a measuring wheel, a linear potentiometer, an accelerometer and a

spring/damper unit. The undulations of the road through the wheel and spring/damper unit cause changes in the length of the linear potentiometer which change its resistance.

Using this measurement system, the MIRA conducted a survey of measuring road profiles over 54 roads across Europe. They came to the important conclusion that the *mean square value* of the displacement and velocity of the road profile taken over a frequency range of 0.005 cycle/ft. (0.0164 cycle/m = 0.103 rad/m) to 0.5 c./ft. (1.64 cycle/m = 103 rad/m) is a good measure of overall *surface roughness* of the road. Although this number provides a "single figure" guide to the roughness of the road, the *power spectral density* (PSD) of the road profile gives more detailed information about it.

Based on the above we choose to use PSD to describe the road of our interest. The concept of stochastic random processes and power spectral density (PSD) is reviewed in the following section.

3.2. A review of stochastic random processes

Probably the most important concept in the theory of probability is the one of *random variables*. In simple terms, a random variable, for example $x(\zeta)$ is the function that assigns a number to each possible outcome of an experience. This number can be voltage of a node in a circuit or the length of a spring. If values are available for an interval of values, the random variable is called *continuous* otherwise it is called a *discrete* random variable [10].

As a simple example, let's assume the experiment of rolling a dice once. The outcome of this experiment can be any integer value between 1 to 6, (i.e. sample space $=\{1,2,3,..,6\}$). We can define an arbitrary random variable $x(\zeta)$ that takes on the value of 1 for odd and 0 for even numbers:

$$x(\zeta) = \begin{cases} 1 & \text{for } \zeta = 1,3,5 \\ 0 & \text{for } \zeta = 2,4,6 \end{cases} \quad \textbf{(3-1)}$$

A *stochastic process* is a rule which assigns every ζ a function x(t,ζ). As an example, the position (relative to a reference point) of any physical point of interest (sample) in a vehicle while being driven on a random road can be represented by a stochastic process, in other words a family (or ensemble) of functions x(t,ζ). In this example $x(t,\zeta_1)$ can represent the position of centre of one specific wheel relative to a reference point [10].

If we assume $x[n]$ as a wide sense stationary discrete process, its *autocorrelation* is defined as:

$$R_{xx}[k] = E(x[n] * x[n-k]) \quad \textbf{(3-2)}$$

3.3. The concept of Power Spectral Density (PSD)

In practical terms, the PSD of a stochastic process is the Fourier transform of the autocorrelation function of the process [11]:

$$S_{xx}(\Omega) \overset{FFT}{\Longleftrightarrow} R_{xx}[k] \quad \textbf{(3-3)}$$

$$S_{xx}(\Omega) = \sum_{k=-\infty}^{+\infty} R_{xx}[k] * e^{-j\Omega \mathrm{k}} \quad \textbf{(3-4)}$$

Aside from the rare obstacles in a road profile, its irregularities or undulations (i.e. change of height) are stochastic in nature [12]. Accepting this fact, Dodds *et al.* suggested that the characteristics of a road profile can be explained using the techniques of theory of random vibrations [12]. This is a very important finding since it enables us to capture the statistical properties of the road using the tools defined with random processes explained above. In what follows I will consider a road profile as a random process and use the concept of power spectral density to describe its characteristics.

A robust road model can define the road as a 3D surface. It can use Cartesian coordinates to describe the surface, z axis pointing in the upward direction, x axis to the front (same as the direction of the car's speed vector) and y axis pointing to the left. At any point in the x-y plane z(x,y) represents the elevation of the road.

Let’s assume a 4-wheel vehicle being driven on this road. The index names "fl", "fr", "rl" and "rr" are used for front left, front right, rear left and rear right wheels respectively. Each wheel will be subject to a different excitation from the road, $z_{fl}(x,y)$, $z_{fr}(x,y)$, $z_{rl}(x,y)$ and $z_{rr}(x,y)$. However assuming that the vehicle is travelling on a direct line then we can safely assume that

$$z_{fl}(x,y)= z_{rl}(x,y) \text{ and } z_{fr}(x,y)= z_{rr}(x,y) \quad \textbf{(3-5)}$$

since wheels on each side (right and left) traverse on the same track.

According to [12] irregularities of road profile fit the category of Gaussian probability distribution. They proved that the assumption of a homogenous and isotropic random process is valid for describing road profiles. They confirmed this hypothesis by extracting the power spectral densities of a left and right tack derived from MIRA's investigation of roads with different roughness indexes [6]. Hence their method proves the possibility of deriving dual track road profiles from a single track road profile measurement [12].

Since a single track road profile is inherited from a dual track model and its statistical characteristics is proven to be the same as any other single track derived from the same road profile, I assume a single track random road profile in this study.

I simplify the model by assuming a single random road profile track, elevation z(s) versus 1-D longitudinal space. The variance of this random process is defined as:

$$\sigma^2 = E\{z_R^2(s)\} = \lim_{X\to\infty}\int_0^X z_R(s)^2 ds \tag{3-6}$$

The variance is a subset of a more general concept, auto-correlation:

$$\begin{aligned} R(\xi) &= E\{z_R(s) * z_R(s+\xi)\} \\ &= \lim_{X\to\infty}\frac{1}{X}\int_0^X z_R(s) * z_R(s+\xi)\, ds \end{aligned} \tag{3-7}$$

Autocorrelation is a tool used for finding repeating patterns. The autocorrelation of a real function is an even function $R(\xi) = R(-\xi)$. The autocorrelation function as its name suggests, and as its Eq. 3-7 shows, finds how similar a signal and its shifted versions are. Hence $R(\xi \to \infty) = 0$, also the maximum of an autocorrelation function happens at $\xi = 0$, which is simply because the most similar shifted version of a function is itself (with no shifts) . The value of $R(0)$ is called the variance or interchangeably autocovariance or σ^2.

In order to find the characteristics of a road profile, it is essential to view it in frequency domain. As stated earlier the Fourier transform of the auto-correlation function coincides with its power spectral density function (PSD):

$$\begin{aligned} S(\Omega) &= \frac{1}{2\pi}\int_0^\infty R(\xi)e^{-i\Omega\xi}\, d\xi \iff R(\xi) \\ &= \int_{-\infty}^{\infty} S(\Omega)e^{i\Omega\xi} d\Omega \end{aligned} \tag{3-8}$$

Note that in the above formula; Ω (wave number) is in rad/m. In order to avoid negative wave numbers, a single sided PSD is preferred (similar to the unilateral Laplace transform). Hence we define the single sided PSD $\Phi(\Omega)$ as follows:

$$\Phi(\Omega) = \begin{cases} 2S(\Omega) & \text{for } \Omega \geq 0 \\ 0 & \text{for } \Omega < 0 \end{cases} \tag{3-9}$$

As mentioned earlier the PSD function for real functions is even, hence the general form of one sided PSD function and its inverse Fourier transform (autocorrelation function) can be simplified as follows:

$$\begin{aligned}&\Phi(\Omega)\\&=\frac{2}{\Pi}\int_0^\infty R(\xi)cos(\Omega\xi)d\xi \overset{Fourier\ Transform}{\Longleftrightarrow} R(\xi)\\&=\int_0^\infty \Phi(\Omega)cos(\Omega\xi)d\Omega\end{aligned} \quad \textbf{(3-10)}$$

Setting $\xi = 0$ in the above formula we get the variance:

$$\sigma^2 = R(\xi = 0) = \int_0^\infty \Phi(\Omega)d\Omega \quad \textbf{(3-11)}$$

Hence the variance (of a real function) can be calculated by integrating the PSD function. In practice we assume the PSD function is given in a certain interval, for instance, $\Omega_{\mathrm{Min}} < \Omega < \Omega_{\mathrm{Max}}$. In a discretely given PSD we can approximate the integral with the sum of the areas between each two point and the horizontal (Ω) axis.

The international standard ISO 8608 "Mechanical vibration - Road surface profiles - Reporting of measured data" provides a standard for reporting one-track and multi-track measurements [5]. It introduces Displacement PSD as a first method of describing a road profile. It also provides us with suggested lower limit and upper limit values of the *wavenumber* with a lower limit of 0.01 cycles/m (0.0628 rad/m) for on-road vehicles and 0.05 cycles/m for off-road vehicles. An upper limit of 10 cycles/m (62.8 rad/m) and 1000 cycles/m (6280 rad/m) is suggested for suspension vibration purposes and for noise purposes respectively. Since the purpose of this study is to estimate the power harvesting potential, noise is not considered a harvestable power source. Hence I use a more

inclusive version of the band recommended for general suspension studies by ISO 8608, from 0.01 rad/m to 100 rad/m, in this study.

3.4. Classification of random road profiles

According to ISO 8608, a road profile PSD can be approximated with the following formula:

$$\Phi(\Omega) = \Phi(\Omega_0) * (\frac{\Omega}{\Omega_0})^{-w} \quad \textbf{(3-12)}$$

$\Phi(\Omega)$ represents the PSD value in units of $m^2/(rad)/m$, equivalently m^3/rad, at each wavenumber Ω which is in units of rad/m. $\Phi_0 = \Phi(\Omega_0)$ is the PSD at the *reference* wavenumber, 1rad/m. The waviness of the road is represented by w.

The ISO 8608 classifies road profiles from A to E according to their degree of roughness, or equivalently their $\Phi(\Omega_0)$. The rougher the road, the higher the PSD value at the wavenumber of 1 rad/m. The waviness (w) reflects the drop in the magnitude of vibrations as well as the PSD of vibrations in higher wavenumbers. After smoothing the PSD from road profile measurements and fitting a curve to it, w is found to be approximately 2. Hence in most studies, same as this thesis, w is considered 2. Class A with Φ_0 equal to $1*10^{-6}$ $m^2/(rad)/m$ represents very smooth highways. Class E with Φ_0=256 $m^2/(rad)/m$, on the other hand, represents very rough roads. The PSD of these standard classes is plotted in Fig 3-1 in the wavenumber range of 0.01 to 100 rad/m.

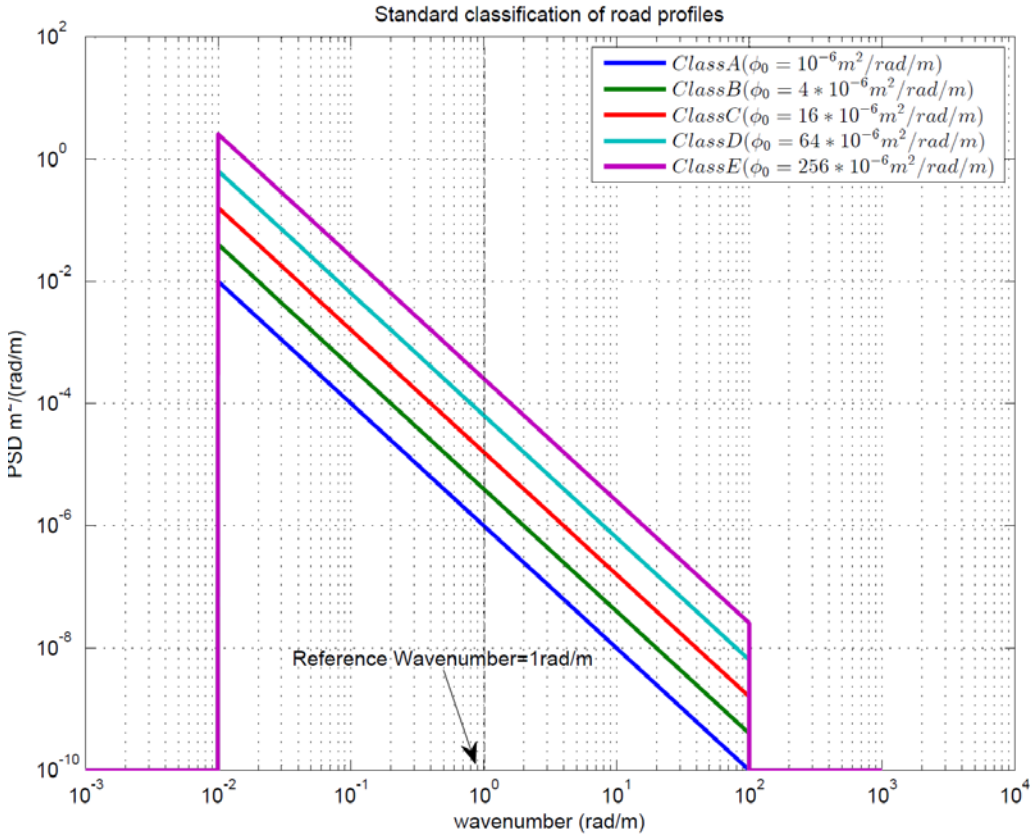

Figure 3-1 Classification of road profiles based on PSD, geometric mean of each class

3.5. Rebuilding a road profile from its PSD

Having the classification of road profiles, I aim to rebuild a random road profile from its given PSD. Power Spectral Density representation of a road profile provides the characteristics of the road in frequency (wavenumber) domain. In order to rebuild the signal I take an approach very similar to that of the inverse Fourier transform.

Fourier transform and its inverse are based on the fact that every signal or function in time can be approximated with superposition of many sinusoidal functions different form each other in frequency and phase properties. This approximation can be ultimately exact, assuming a sum of infinite number of sinusoidal functions.

Let's decompose a road profile in terms of sum of infinite N sine functions with frequencies (or wave number in case of road profile) Ω_i, phases Ψ_i and amplitudes of A_i.

$$z_R(s) = \sum_{i=1}^{N} A_i \sin(\Omega_i s - \Psi_i) \tag{3-13}$$

The variance of the road profile using the right side of the above mentioned formula is [11]:

$$\sigma^2 = \lim_{X\to\infty} \frac{1}{X} \int_0^X \left(\sum_{i=1}^{N} A_i \sin(\Omega_i s - \Psi_i)\right) * \left(\sum_{j=1}^{N} A_j \sin(\Omega_j s - \Psi_j)\right) ds \tag{3-14}$$

for $i = j$ and $i \neq j$ this integral is simplified differently, for $i = j$ we have

$$J_{ii} = \int A_i^2 \sin^2(\Omega_i s - \Psi_i) ds = \frac{A_i^2}{2\Omega_i}\left[\Omega_i s - \Psi_i - \frac{1}{2}\sin(2(\Omega_i s - \Psi_i))\right] \tag{3-15}$$

for $i \neq j$

$$J_{ij} = \int A_i \sin(\Omega_i s - \Psi_i) * A_j \sin(\Omega_j s - \Psi_j) \tag{3-16}$$

$$= \frac{1}{2} A_i A_j \left(\int \cos((\Omega_i - \Omega_j)s - (\Psi_i - \Psi_j)) ds - \int \cos((\Omega_i + \Omega_j)s - (\Psi_i + \Psi_j)) ds\right) \tag{3-17}$$

$$= \frac{1}{2} A_i A_j \left(- \frac{\sin((\Omega_i - \Omega_j)s - (\Psi_i - \Psi_j))}{(\Omega_i - \Omega_j)} + \frac{\sin((\Omega_i + \Omega_j)s - (\Psi_i + \Psi_j))}{(\Omega_i + \Omega_j)} \right) \quad \textbf{(3-18)}$$

Hence

$$\sigma^2 = \lim_{X \to \infty} \frac{1}{X} \int_0^X \sum_{j=1}^{N} J_{ii} + \lim_{X \to \infty} \frac{1}{X} \int_0^X \sum_{j=1}^{N} J_{ij} \quad \textbf{(3-19)}$$

$$= \frac{1}{2} \sum_{i=1}^{N} A_i^2 \quad \textbf{(3-20)}$$

From Eq. 3-11 we found that the variance of the road profile using the area under (integral of) the PSD diagram. Using this fact and the result driven above the amplitudes A_i can be calculated as [11]

$$A_i = \sqrt{2\Phi(\Omega_i)\Delta\Omega} \quad , \qquad i = 1,2,\dots N \quad \textbf{(3-21)}$$

Since I assumed that only the PSD information of the original road profile is available, it is not possible calculate the phases from its PSD. Hence I assume a random distribution of phases from 0 to 2π.

Using the theory explained in this chapter I developed a function in MATLAB (provided in Appendix A) that generates a road profile realization of a given road profile PSD. Figures 3-2 to 3-4 show *a realization* for each of the standard classes of road classes outlined by ISO 8608.

Please note that this code uses the function *rand* to generate uniformly distributed numbers between 0 and 2π for Ψ_i, hence running the code multiple times will not lead to same road profiles, but the road profiles generated for a specific class have the same *statistical properties* or in practical terms they have very similar PSDs. I have tested this idea using a reverse approach of generating a road profile from a PSD and then

reproducing the PSD from the road profile to ensure that the road profiles generated are a suitable representative for each road profile class A to E.

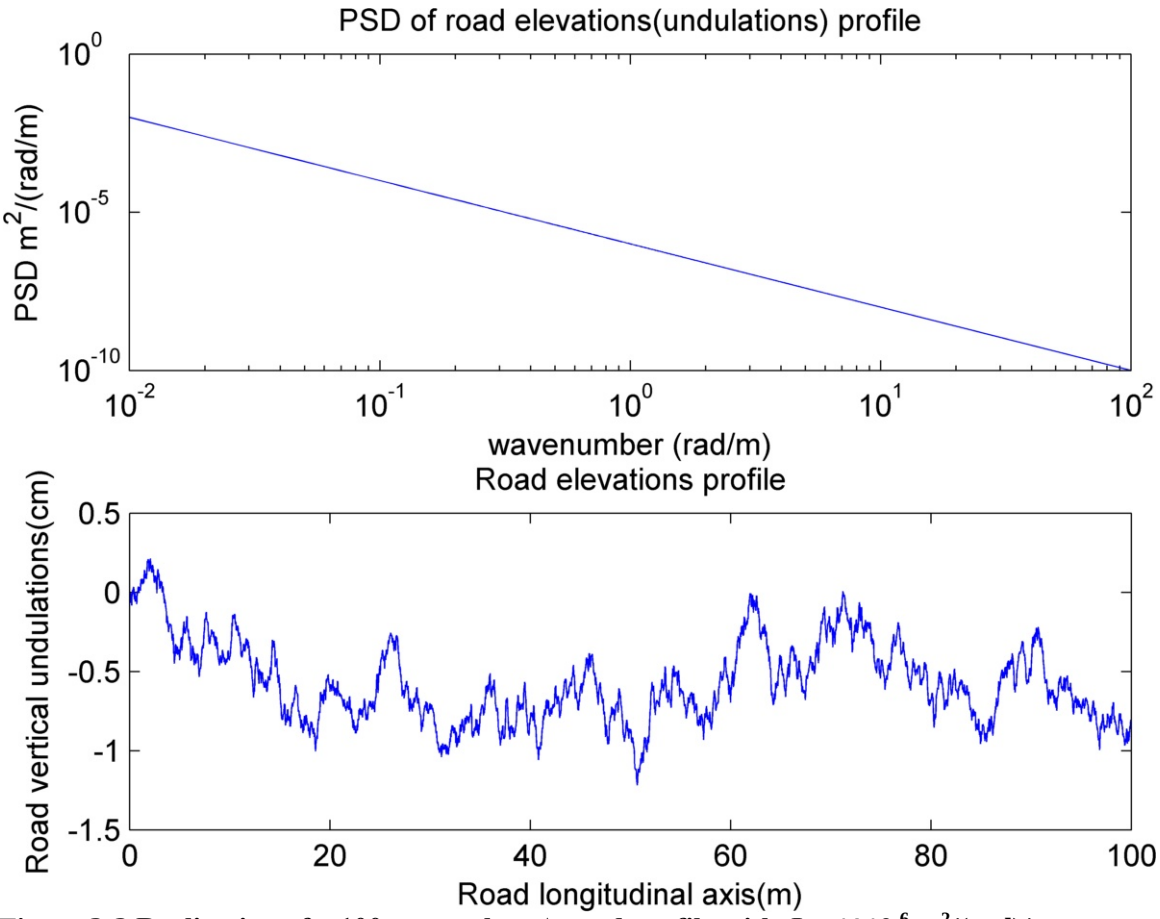

Figure 3-2 Realization of a 100 meter class A road profile with $\Phi_0=1*10^{-6}$ $m^2/(rad)/m$

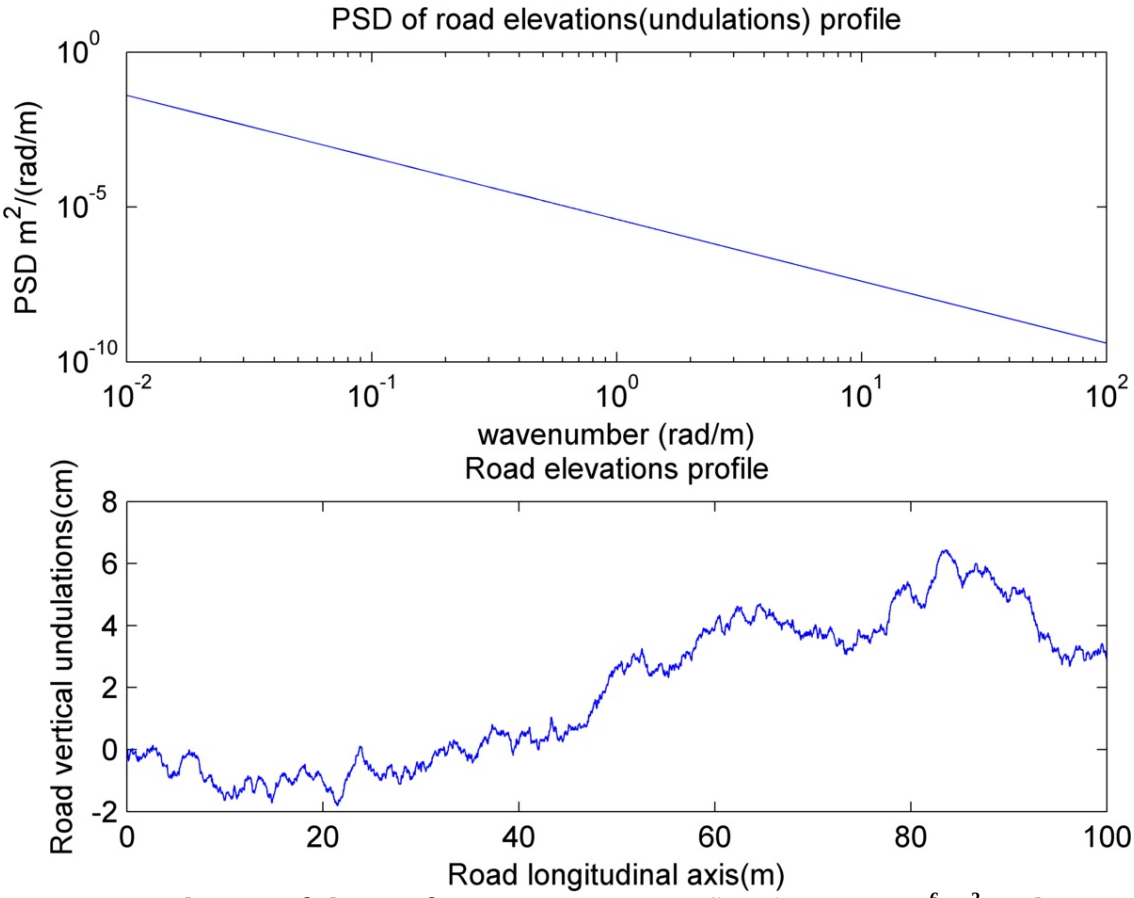

Figure 3-3 Realization of class B of a 100 meter road profile with $\Phi_0=4*10^{-6}$ $m^2/(rad)/m$

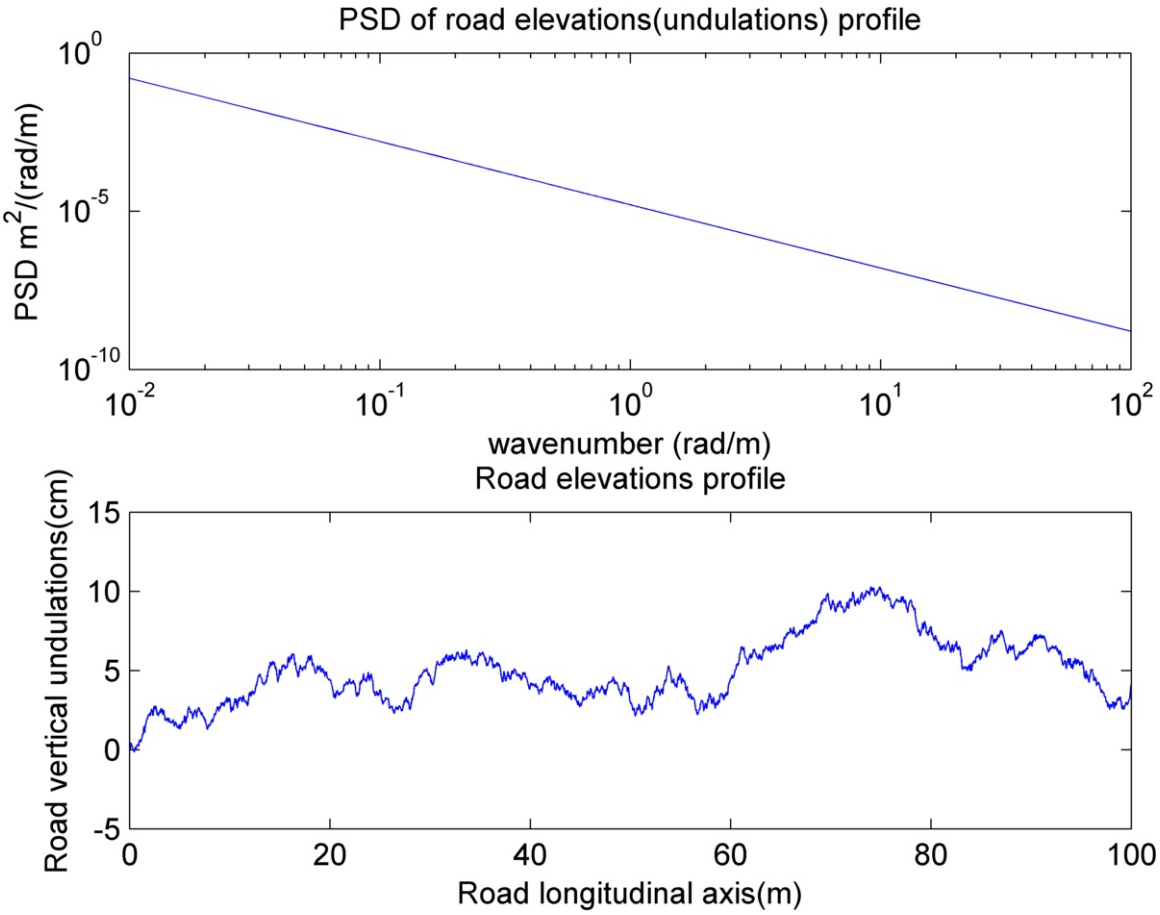

Figure 3-4 Realization of class B of a 100 meter road profile with Φ0=16*10-6 m2/(rad)/m

In Chapter 4, I will use the road profiles generated in this section as an input to the simulator of the dynamics of the suspension system of a vehicle using the 2-DOF model introduced in Chapter 3.

Chapter 4

Simulation Results

In Chapter 2 and 3, I described the approach to modeling the dynamics of the vehicle and the road profile. I deployed these two models in order to find the power harvesting potential in a conventional vehicle viscous damper. Assuming that a regenerative alternative of viscous dampers is to be designed for passenger vehicles, the results in this chapter provide us with an idea of *how much* and in *what form* this power would be.

Using the models of road profile and 2-DOF quarter car model and the power dissipation formula for the viscous damper, we can now run simulations for a vehicle traversing with a constant speed v (km/h) on a road with a specific degree of roughness $\Phi(\Omega_0)$ and length of L2-L1. The vehicle model has a set of characteristics such as sprung and unsprung mass damper and spring stiffness and tire stiffness. I set these parameters to the following values that have been used in several other studies [13] [14] [15].

Table 4.1 Parameters of the 2-DOF quarter car used for modeling

Parameter	Value
Sprung mass (m_1)	343.75 kg
Unsprung mass (m_2)	40 kg
Suspension stiffness (k_1)	20053 N/m
Tire stiffness (k_2)	182087 N/m
Suspension damping coefficient (c_1)	1388 Ns/m
Tire damping coefficient (c_2)	0 Ns/m

A set of possible vehicle speeds is assumed which are maximum allowed driving speeds in Canada [16]. These speeds are classified in the Table 4-2. However for graphs,

an extended set of speeds, from 10Km/h to 120Km/h in increments of 10km/h has been considered.

Table 4.2 Typical maximum allowed driving speeds in Canada

Type of road	Maximum allowed speed in Canada
Multi-lane highways and expressways	100 Km/h
Two-lane highways	100 Km/h
Major roads in urban areas	60 Km/h
Residential areas	50 Km/h
Near schools and playgrounds	30 Km/h

Figure 4-1 shows the output of the simulation for a vehicle traveling at the speed of 60km/h on a class C road (Φ_0=16 m^2/(rad)/m).

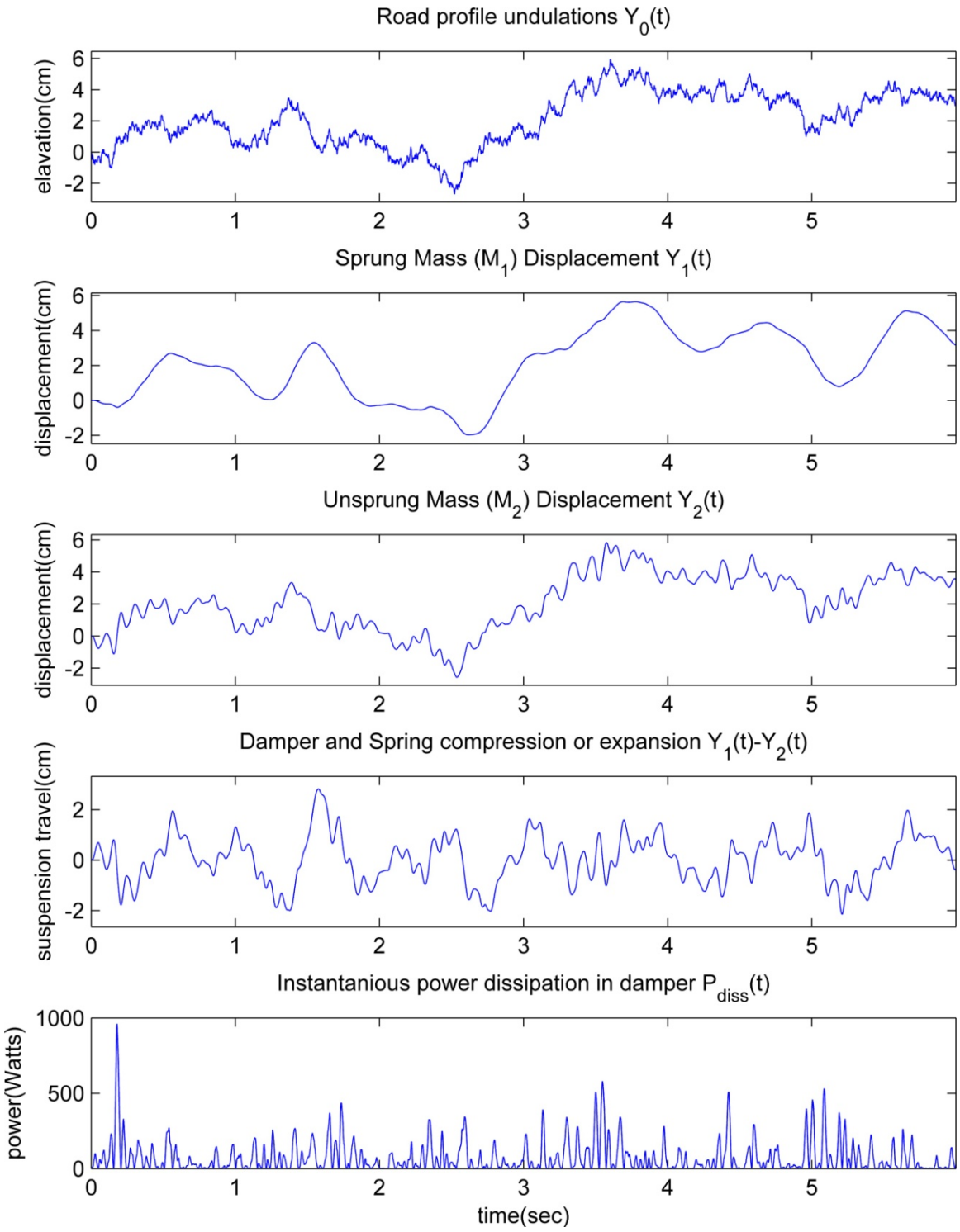

Figure 4-1 Simulation results for the road profile elevations, sprung mass and unsprung mass vertical displacements, suspension travel and instantaneous dissipated power in the damper

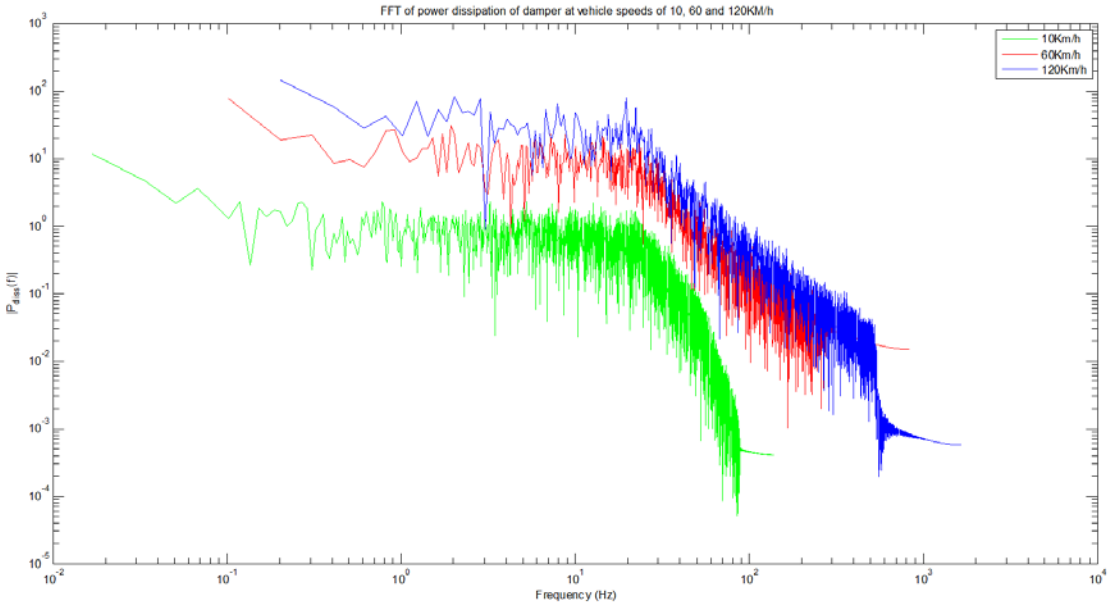

Figure 4-2 FFT of power dissipation of damper at vehicle speeds of 10Km/h, 60 Km/h and 120 Km/h at a class C road

As Fig. 4-2 shows, moving towards higher speeds, the power dissipation at the viscous damper shifts to higher frequencies. Most of the available power harvesting potential seems to be at frequencies approximately less than 100 Hz. This information can be used in optimizing the design of power converters which condition the power output of the electric regenerative damper into a power that can charge batteries.

4.1. Parameter sensitivity analysis

The dissipated power in the damper is dependent on the characteristics of the damper, road profile roughness and speed of the vehicle. In this section I am interested to find the sensitivity of power dissipation to these parameters.

It is worth noting that since each run of the simulator makes a random road profile with the characteristics defined by an specific PSD but using random phases, for each parameter change, I run the simulation for a number of times (variable '*reps*' in the

MATLAB code) and then report the average of results. I use reps=10 in this work unless otherwise mentioned. This number has been achieved by the method of trial and failure to ensure that the achieved power from each run of the simulator for a specific road roughness degree and vehicle speed does not vary from another run's achieved power by more than 1%.

In Table 4-3 I report the power dissipations in the viscous damper found by the simulations. I ran the simulations for different road profile roughness degrees for the speed limits in Canada. The dissipated power in the damper in terms of mean and RMS is reported in the table below.

Table 4.3 Simulation results of power dissipation in the damper

	30 km/h		**50 km/h**		**60 km/h**		**100 km/h**	
Φ_0 (m^2/rad/m)	**Mean** (W)	**RMS** (W)	**Mean** (W)	**RMS** (W)	**Mean** (W)	**RMS** (W)	**Mean** (W)	**RMS** (W)
1E-6 (Class A)	2.4	4.1	4.1	7.2	5	8.6	7.6	13.2
4E-6 (Class B)	9.9	17.2	15.9	27.2	18.4	32.2	30.6	52.9
16E-6 (Class C)	38.4	66	65	111.9	74.8	127.5	122.5	210.6
64E-6 (Class D)	157.8	276.1	258	448.5	291.5	510	501.9	856.2
256E-6 (Class E)	627.9	1090.4	997.7	1733.2	1215.7	2105.8	2113.2	3546

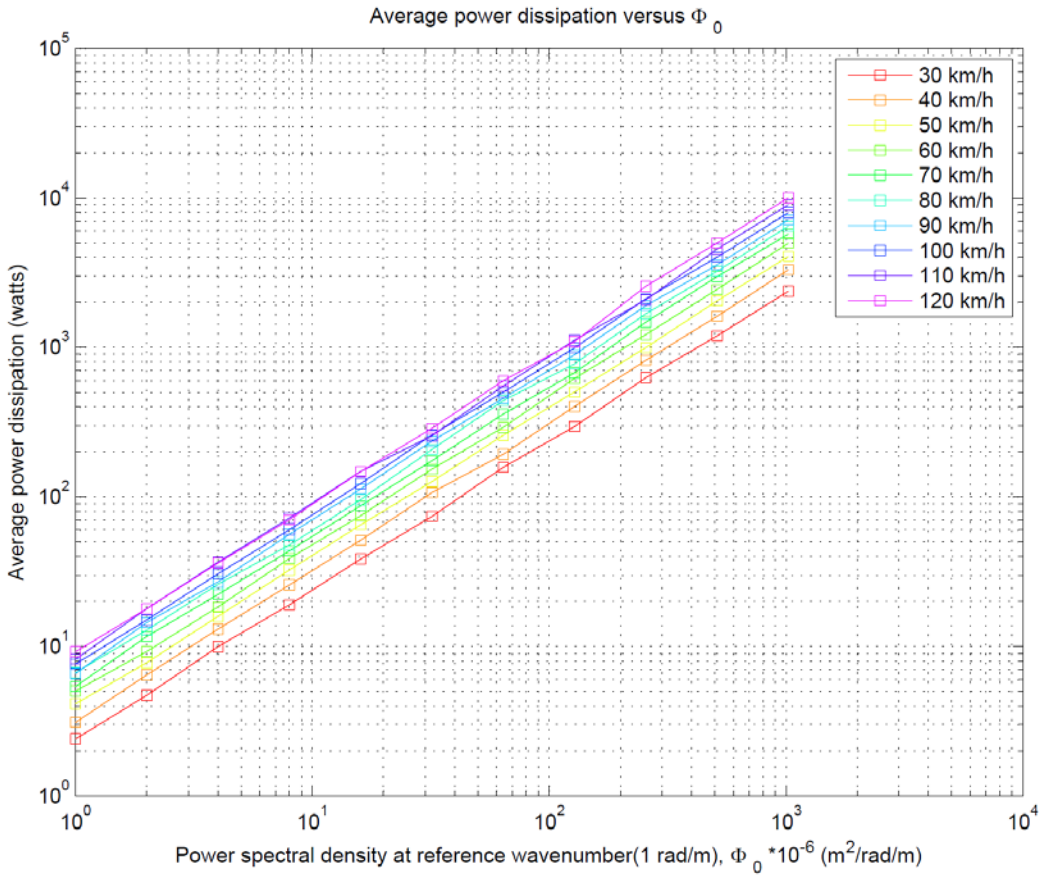

Figure 4-3 Average dissipated power vs. PSD for different driving speeds

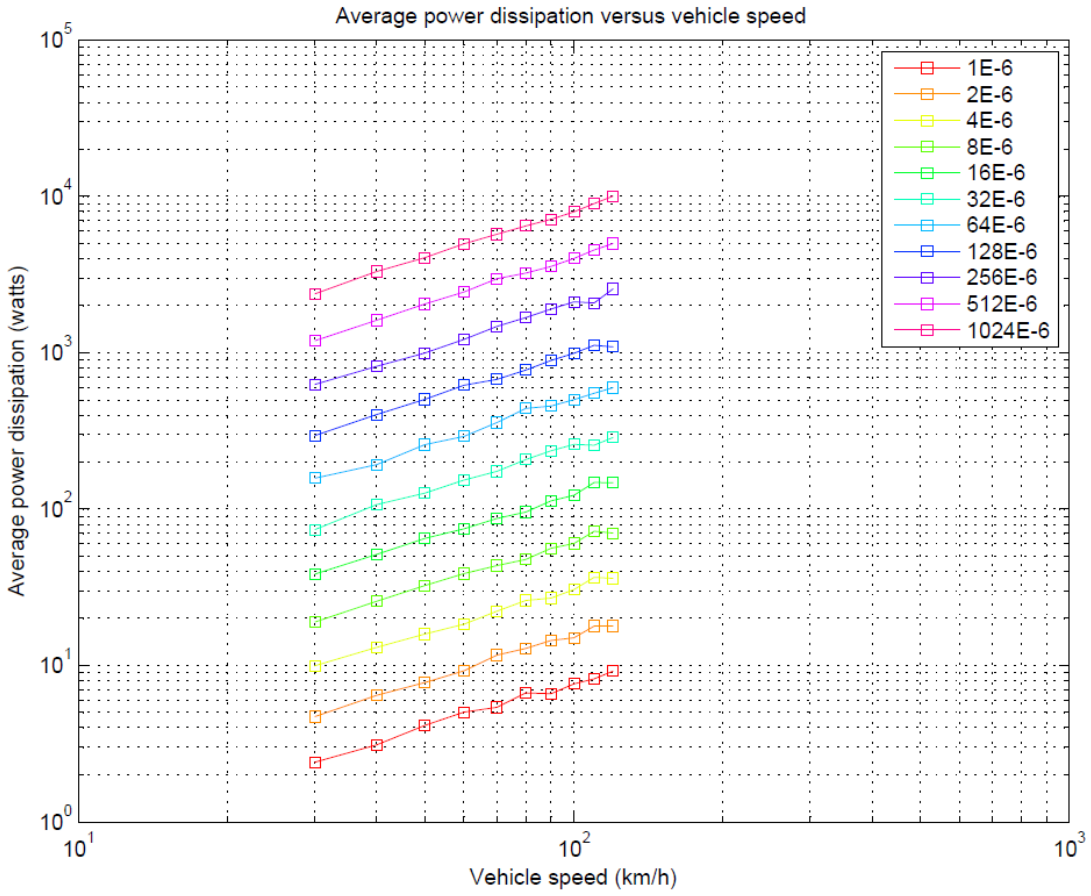

Figure 4-4 Average power dissipation vs. vehicle speed for different road roughness degrees

Chapter 5

Power harvesting from electric dampers

In Chapter 2, new technologies such as active and semi-active suspensions were introduced. These technologies aim to improve the performance of conventional suspension systems. One of the issues aligned with these new technologies is their high power consumption. This arises from the need to generate dynamically controlled force in the active suspension systems as opposed to conventional suspension systems which use passive elements such as spring and damper which have fixed characteristics and do not require an electric power supply.

In order to generate the dynamic force required several alternatives for the actuator have been proposed. All active suspensions proposed use an active element as the actuator. The best alternative for such an actuator seems to be an electric motor. A DC motor can respond to the controller commands very fast and is also lighter than other alternatives such as a flywheel.

The active damper requires an actuator that can produce translational motion (and force), however most commercially available DC motors generate torque. Hence in order to convert the torque to translational movements a mechanical converter (such as ball-screw) should be used.

A ball-screw is a mechanical device designed to convert rotational motions to linear and vice versa. It is used in almost every car that features power steering system in order to convert the rotary motion of the electric machine into linear motion of the steering rack.

Suda *et al* has considered a ball-screw system to convert the translational movements of the wheel into rotational force to harvest energy through the rotor of a DC machine. Other recent technologies such as the linear DC machine (Fig 5-2) are designed to be used as electric dampers [17].

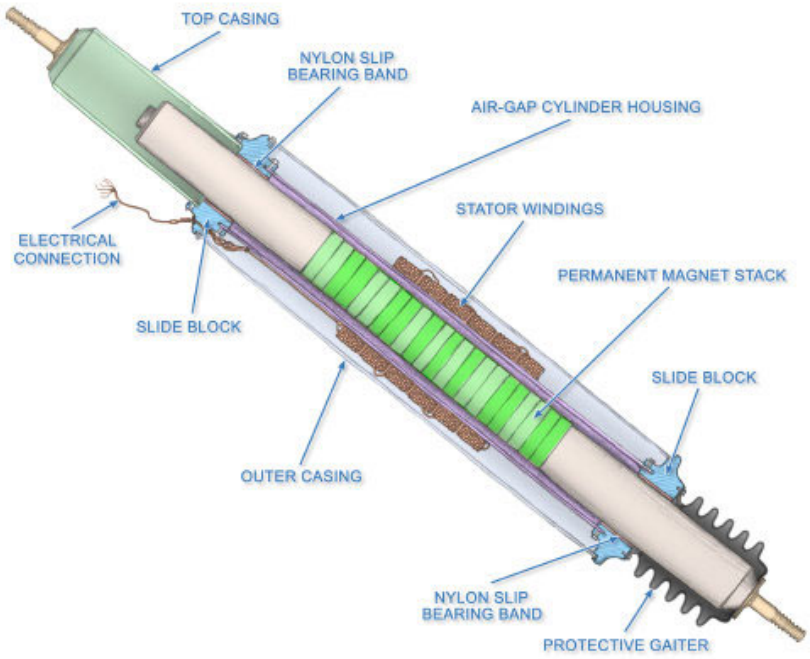

Figure 5-1 Linear DC motor technology, picture from [18]

Having an electric DC machine in the suspension system, the idea of power harvesting from the suspension system of vehicles has been of interest in the last two decades. Several research papers have been published proposing "self-powered" active suspension systems [19].

In the previous chapter using the simulator of the vehicle dynamics and road profile I simulated the power dissipation in a conventional viscous damper or in other words I found the power harvesting potential of the damper of vehicles' suspension system.

The idea used in thesis is that, if such an ideal electric actuator exists that can generate the same reaction force to that of a conventional damper with damping coefficient c and

hence generate force of $F_d = c(v_2 - v_1)$ and can convert this power from mechanical form of vibrations to electrical form, then the same amount of power can be harvested using this actuator that would be wasted otherwise in the damper.

In this chapter, I assume that such an ideal electric damper is used as an actuator, which can generate the same power as found otherwise being wasted in the viscous damper in Chapter 4. However, even considering this ideal electric damper, the problem of irregularity of its output power exists. This is because of the fact that road profiles are of random nature and thus as shown earlier in Figure 4-1, the output power is not constant. The output power of the regenerative damper can vary anywhere from 0 to maximum for a specific road profile (with a specific PSD) and a specific driving speed for a car.

Figure 5-2 shows an overall diagram of the regenerative active suspension system considered in this study. The controller decides the operating mode of the system by monitoring the inputs, such as the accelerometers, battery's stage of charge and the user preference. The accelerometers output, after applying signal processing methods, indicate the degree of roughness of the road profile. The user preferences include battery saving mode or high performance modes of best handling performance or best comfort.

The controller chooses between regenerative mode and active mode. The electric actuator is controlled in each mode by the PWM wave produced by the controller. Power can flow both ways as shown in Fig 5-2, to and from the battery, indicating regenerative and active mode of operation respectively.

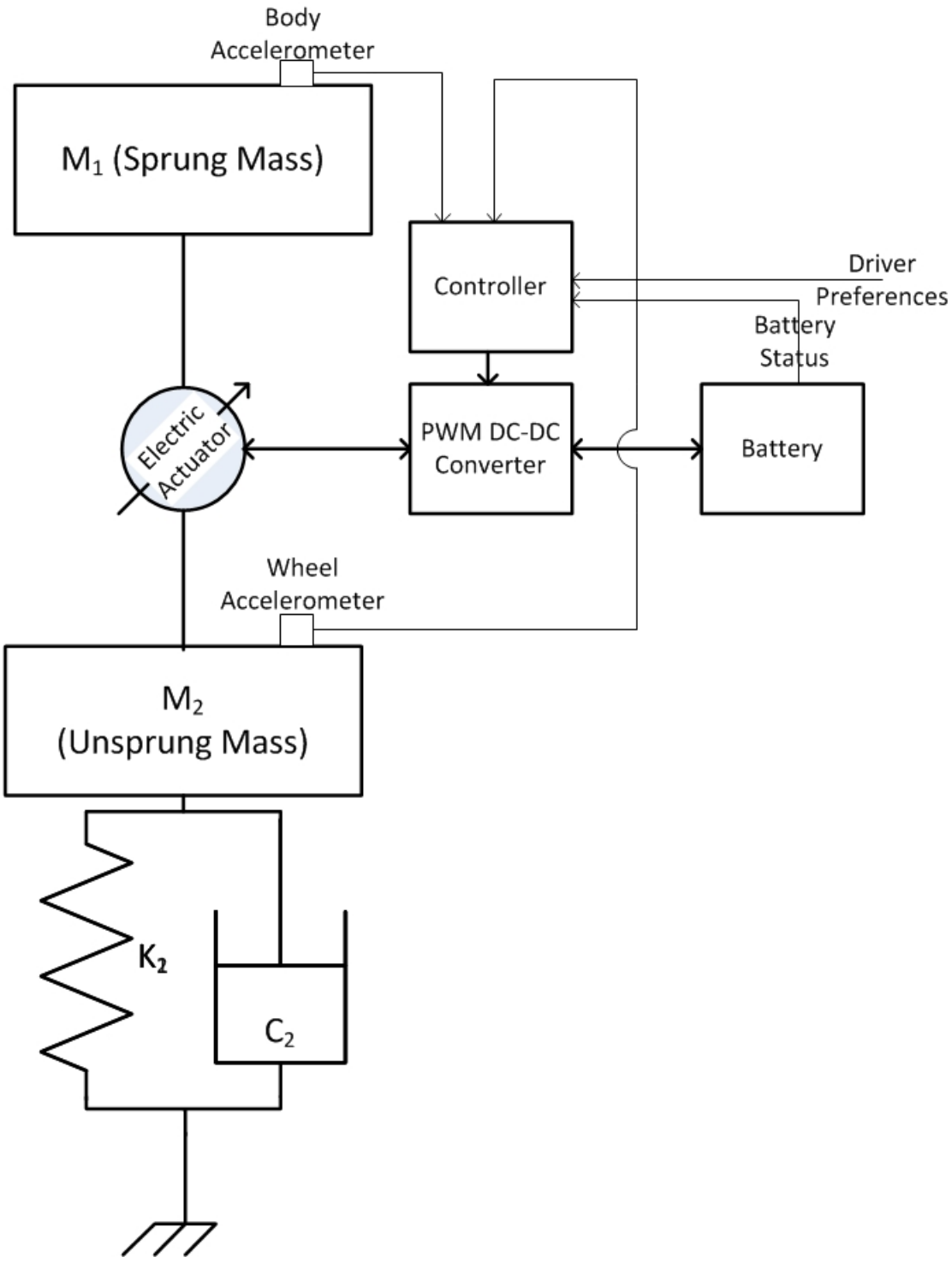

Figure 5-2 Overview of the regenerative active suspension system

In this chapter, I focus on the problem of varying output power of regenerative electric dampers and propose a power conditioning system designed to convert the output power of the electric damper into a form that can be stored in a condenser or a storage device. I start by reviewing types of storage devices used in passenger cars and a brief review of PWM DC-DC converters.

5.1. Types of storage used in passenger cars

Batteries are essential parts of every vehicle. Their main role is to provide the initial energy for ignition spark in Internal Combustion Engine (ICE) motor vehicles. Most passenger cars which have ICEs use Lead-acid battery as their main electric storage device. However hybrid electric vehicles (HEVs) and electric vehicles (EVs) have higher power requirements which Lead Acid battery is not capable of delivering that power. EVs and HEVs use nickel metal hydride (NiMH) batteries or lithium-ion (Li-ion) batteries which have higher energy density and power density than Lead-Acid batteries.

Each of these batteries has a specific operating voltage and design of the battery system. Conventional ICE cars use 12 V Lead acid battery while the EVs and HEVs battery packs output potential is up to hundreds of volts. These batteries use an integrated control system for charging and converting the power to three-phase to run the AC motors.

5.2. Brief review of Pulse -Width Modulation (PWM) DC-DC converters

DC-DC power converters are used in many applications and the majority of electronic devices, such as laptops cell phones and devices which incorporate DC motor control advantage from one or several PWM DC-DC converters.

A PWM DC-DC converter uses an active switching device like a BJT or MOSFET transistor in order to control the power flow from a DC input to the DC output. The control of the switch is handled by a square waveform called Pulse-Width Modulated (PWM) which controls the state of the switch (ON or OFF) by applying the proper voltage level to the control input (e.g. gate in a MOSFET) of the switch.

Basic PWM DC-DC converters types are *buck, boost* and *buck-boost,* which are used in applications where the output voltage needs to be lower (buck), higher (boost) and either lower or higher (buck-boost) than the DC level of the input voltage.

The output voltage of all PWM DC-DC converters is controlled by the duty cycle (D) of the PWM signal. D is defined as the ratio of ON time of the switch to the period of the PWM signal:

$$D = \frac{t_{on}}{t_{off} + t_{on}} = \frac{t_{on}}{T} \qquad \textbf{(5-1)}$$

The level of output DC voltage of the buck, boost and buck-boost converter in steady state conditions as a function of D and assuming ideal components with no loss are as follows: [20]

Table 5.1 Basic types of PWM DC-DC converter

DC-DC converter type	$\boldsymbol{M(D) = \frac{\text{Vout}}{\text{Vin}}}$
Buck (step-down)	$M(D) = D$
Boost (step-up)	$M(D) = \frac{1}{D}$
Buck-Boost	$M(D) = \frac{-D}{1-D}$

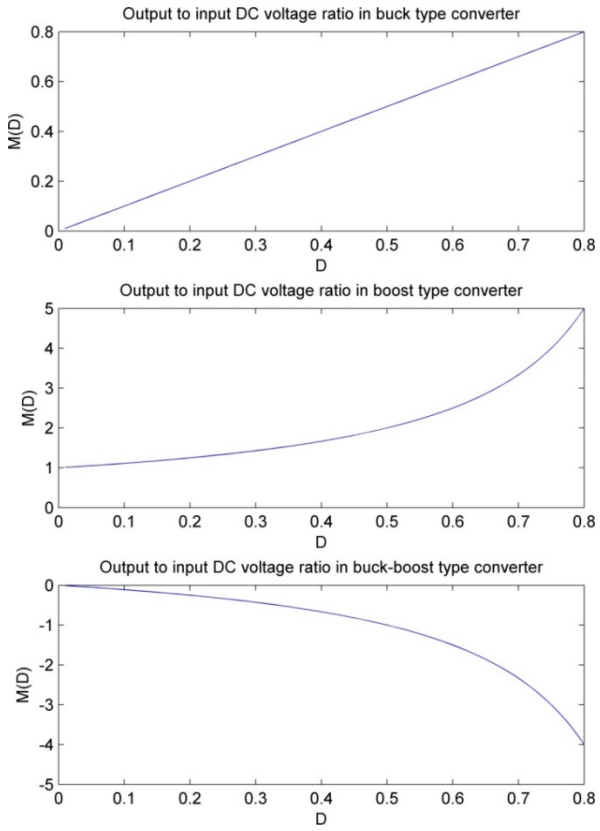

Figure 5-3 Conversion ratios of buck, boost and buck-boost converter as a function of D, $\mathbf{M(D) = \frac{Vout}{Vin}}$

5.3. Dead-zone of regenerative suspension and boost converter as a solution

Okada *et al.* [21] have proposed using the boost type DC-DC power converter in order to use the power harvesting potential in the *dead zone* state of the regenerative suspension. Dead zone corresponds to the states in which the electric machine's output voltage is less than the voltage potential level of the storage (battery). This means that the regenerative suspension is *not* able to charge the battery directly. Harvesting power from the dead zone keeps the regenerative suspension electrically loaded which also means that the regenerative suspension will be producing force even when the relative travel velocity of the damper is less than minimum.

5.3.1. PWM DC-DC converter loaded by a resistance

Having the idea of regenerating power from the electric active suspension even when operating in dead zone as an initial motivation, I have designed and modeled a boost-type PWM DC-DC power converter in Cadence Capture environment using discrete analog elements.

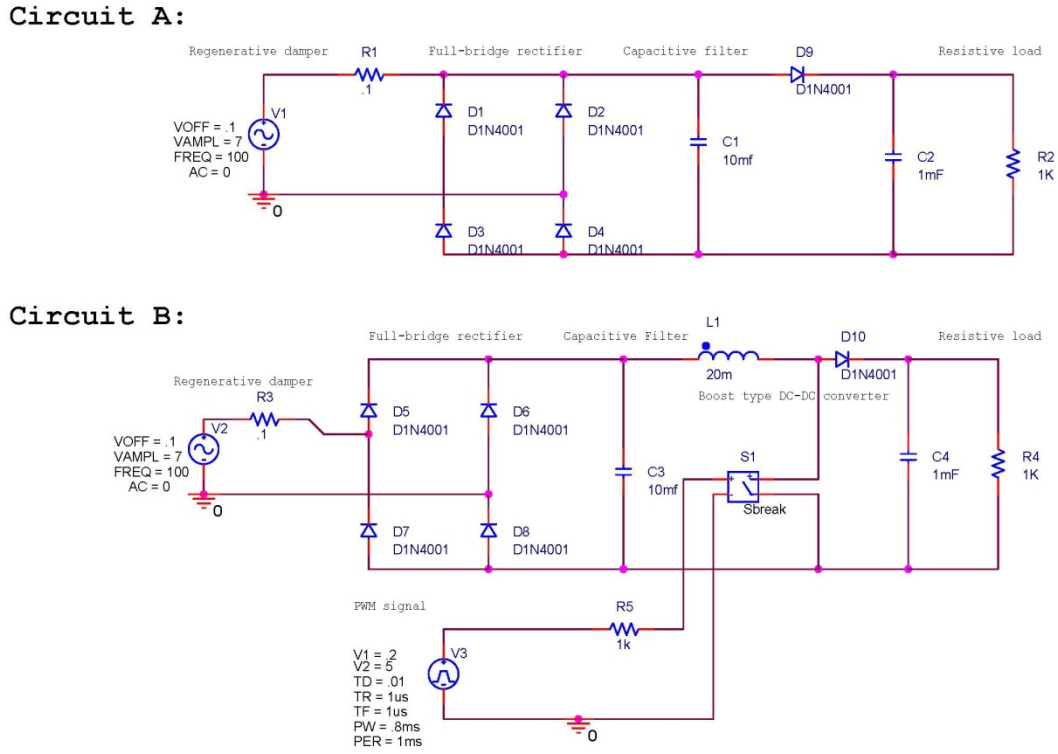

Figure 5-4 Circuit diagram of regenerative damper without and with DC-DC Converter serving a resistive load

Circuit A models a regenerative damper with a sinusoidal output voltage of 7 volts, connected to a resistive load through full-bridge rectifier and capacitive filter.

Circuit B shows the implementation of boost type DC-DC converter using an ideal switch (including inductance L1, switch S1 and diode D5). PWM waveform is generated

using V7 which has an ON time of 0.8ms and an off time of 0.2ms. Hence $D = \left(\frac{0.8\ ms}{0.8+0.2\ ms}\right) = 0.8$. The rectifier and capacitor filter provide the input to the DC-DC converter. On the output we assumed a resistive load (R2=1k) and a large capacitor (C4=1mF) for further filtering of harmonics.

I assumed a regenerative electric damper that can generate electric power with a maximum potential of 12 Volts. In order to simulate the dead-zone problem, I assumed a pure sinusoidal input waveform with amplitude of 7 volts (less than max and less than the battery level) and frequency of 100 Hz for both circuits. This input voltage sources (V1 and V2) mimic the output of a DC regenerative damper operating in dead zone. In other words the damper's relative velocity is not enough to charge the battery directly. In what follows, I test the performance of the proposed boost converter in such condition.

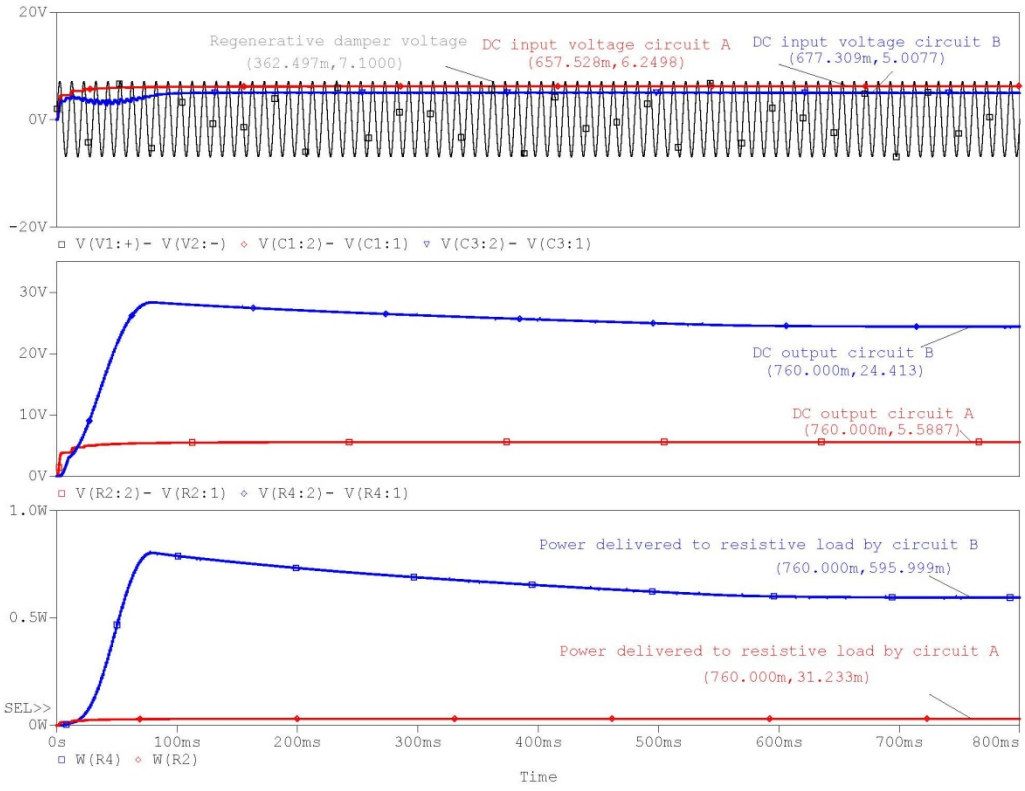

Figure 5-5 PSpice simulation results of regenerative damper without and with DC-DC Converter serving a resistive load

Figure 5-4 shows the simulation results for circuit A and B.

Circuit A, is only able to extract the DC component of the regenerative damper, producing an output of 5.58 volts.

According to theoretical output to input voltage ratio of PWM DC-DC boost type converter outlined in Table 5-1, circuit B is expected to have an output to input voltage ratio of $M(D = 0.8) = \frac{1}{1-0.8} = 5$. The simulation results agree with the theory very closely, $\frac{V_{out}}{V_{in}} = \frac{V_{R4}}{V_{C3}} = \frac{24.41}{5.58} = 4.37$. The internal resistance of the regenerative damper (R6) and the voltage drop of V(on) of D5 explain the difference between the theory and simulation results.

The output power dissipated at the resistive load is increased from 31.23mW in circuit A to 595.99mW in circuit B because of the higher output voltage of the circuit with PWM DC-DC boost converter.

5.3.2. PWM DC-DC converter charging a battery

In this simulation, I replace the resistive load with a 12V battery with an internal resistance of 0.2 Ohms and run the simulation again in order to analyze the performance of the PWM DC-DC power converter in charging the vehicle battery in the case in which the electric damper is operating in dead-zone.

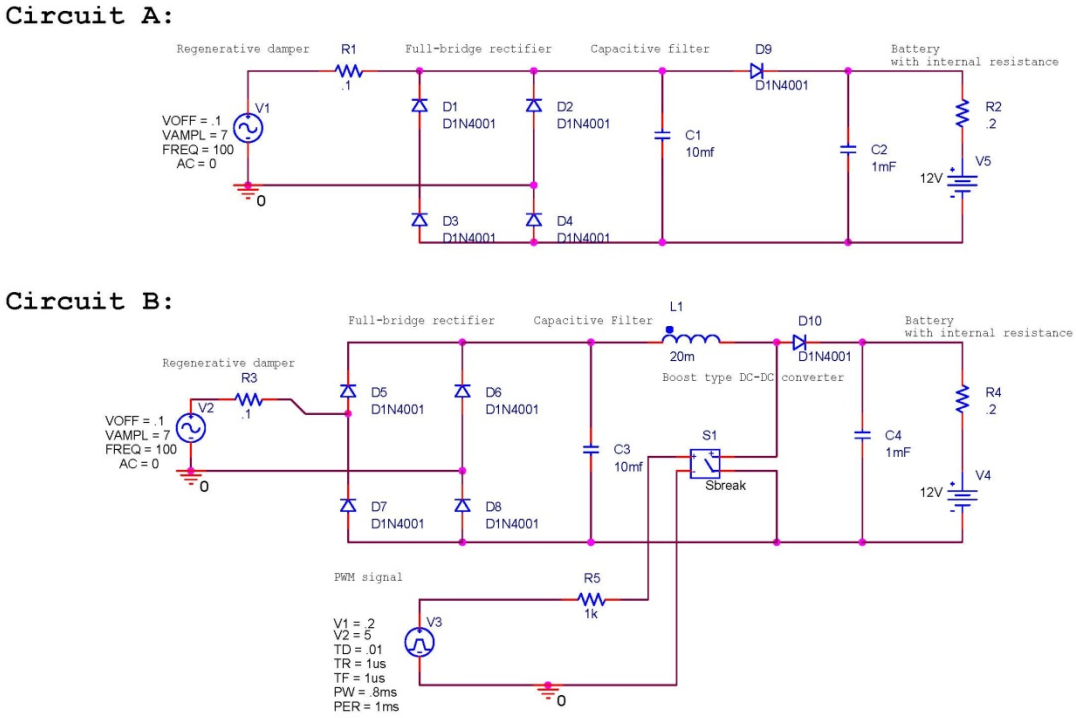

Figure 5-6 Circuit diagram of regenerative damper without and with DC-DC Converter charging a 12V battery

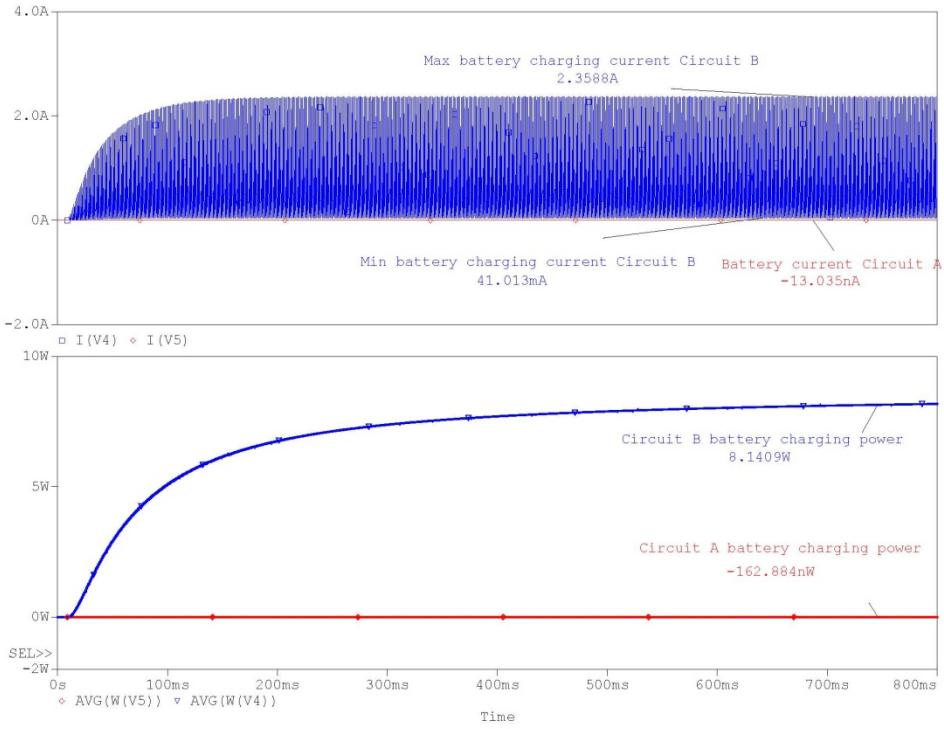

Figure 5-7 PSpice simulation results of regenerative damper without and with DC-DC Converter charging a 12V battery

The output of the simulation shows that while circuit A was not able to charge the battery when the regenerative damper was in dead zone, circuit B charged the battery at the rate of 8.1 Watts.

Chapter 6

Conclusions and future work

In this thesis I introduced the idea of power harvesting from an electric damper used in active suspension systems.

I modeled a vehicle using a 2-DOF quarter car model along with its equations of motions and analytical formula for calculating power dissipation in a conventional viscous damper.

I took a closer look into road profile undulations being the source of vibrations that take place in the vehicle's suspension system. I modelled the road profile using theory of random processes and according to ISO 8608. I combined the model of 2-DOF quarter car and road profile and developed a simulator which reports dynamics of the entire system and mainly the power dissipations of the damper.

Analyzing the results, I learnt that the power dissipation of the damper is also random and varying. Assuming a regenerative damper which is aimed to harvest the power that would otherwise be wasted in a viscous damper, I introduced the problem of dead zone operation of the electric damper. I deployed PWM DC-DC damper to overcome this problem, and tested this theory with circuit level simulations.

6.1. Future work

In this thesis, I tackled several problems which open doors to several research goals in the fields of electrical engineering and automotive industry in the future.

I aim to enhance the models of vehicle dynamics and also road profile to have a more accurate measure of power harvesting potential of the system. I am motivated to look into

other power loss sources of the vehicle, such as the heat loss in the engine, exhaust and brakes.

I believe that a control system, depicted in Fig 5-2, will reveal the potential of power harvesting potential of the regenerative damper and also contribute to its operation in active mode. Hence, I plan to further expand this research to include the control system design for the electric damper and PWM power converter.

Bibliography

[1] International Energey Agency, "World Energy Outlook," 2011.

[2] International Energy Agency, "Transport, Energy and CO2," 2009.

[3] Intergovernmental Panel On Climate Change, "Implications of Proposed CO2 Emissions Limitations," 1997.

[4] Office of Transportation and Air Quality, U.S Department of Energy, "Fuel Economy," U.S Department of Energy website, 14 November 2013. [Online]. Available: http://www.fueleconomy.gov/feg/atv.shtml.

[5] International Organization for Standardization (ISO), *International Standard ISO 8608: Mechanical vibration - Road surface profiles - Reporting of measured data*, 1995.

[6] R.P. La Barre; R. T. Forbes; S.Andrew, "The Measurement and Analysis of Road Surface Roughness," The Motor Industry Research Association, 1975.

[7] C. J. Longhurst, "The suspension bible," CarBibles, [Online]. Available: http://www.carbibles.com/suspension_bible.html. [Accessed 17 11 2013].

[8] Elsayed M. Elbeheiry; Dean C. Karnopp; Mohamed E. Elaraby; Ahmed M. Abdelraaouf, "Advanced ground vehicle suspension systems - A classified bibliography," *Vehicle system dynamics*, no. 24, pp. 231-258, 1995.

[9] S. G. Kelly, Mechanical Vibrations: Theory and Applications, Cengage Learning, 2012.

[10] A. Papoulis and S. Pillai, Probability, Random Variables and Stochastic Processes, McGraw-Hill Science, 2002.

[11] G. Rill, Road Vehicle Dynamics: Fundamentals and Modeling, CRC Press, 2011 .

[12] C. Dodds and J. Robson, "The description of road surface roughness," *Journal of Sound and Vibration*, no. 31, pp. 175-183, 1973.

[13] H. Kim and Y.-S. Yoon, "Semi-Active Suspension with Preview using a Frequency-Shape Performance," *Vehicle System Dynamics: International Journal of Vehicle Mechanics and Mobility*, vol. 10, no. 24, pp. 759-780, 1995.

[14] L. Zuo and S. A.Nayfeh, "Structured H2 optimization of a vehicle suspensions based on multi-wheel models," *Vehicle Systems Dynamics*, vol. 40, no. 5, pp. 351-371, 2003.

[15] L. Zuo and P.-S. Zhang, "Energy harvesting, ride, comfort, and road handling of regenerative vehicle suspensions," *Journal of Vibration and Acoustics*, vol. 135, 2013.

[16] "Roads Types and Speed Limits," Angloinfo Canada, [Online]. Available: http://canada.angloinfo.com/transport/driving/roads-speed-limit/. [Accessed 17 November 2013].

[17] Y. Suda, Nakano K. et al., "Study on Electromagnetic Suspension for Automobiles-simulation and Experiments of Performance," in *International Symposium on Advanced Vehicle Control*, Ann Arbor, Michigan, 2000.

[18] J. Ramsey, "On the Rebound: Scientists invent regenerative shocks," Autoblog, 1 February 2009. [Online]. Available: http://www.autoblog.com/2009/02/01/on-the-rebound-scientists-invent-regenerative-shocks/.

[19] M. Fodor and R. Redfield, "The Variable Linear Transmission for Regenerative Damping in Vehicle Suspension Control," in *American Control Conference*, Chicago, 1992.

[20] R. W. Erickson and D. Maksimovic, Fundamentals of power electronics, New York: Kluwer Academic Publishers, 2004.

[21] Y. Okada, S.-S. Kim and K. Ozawa, "Energy Regenerative and Active Control Suspension," in *ASME Design Engineering Technical Conferences (DETC'03)*, Chicago, 2003.

[22] International Organization for Standardization, "Mechanical vibration - Road surface profiles - Reporting of measured data," 1995.

Appendix A

MATLAB Code for generating a random road profile

```
% The function genprofile(PSI0,plot1,L) generates a random
road profile with the length of L, and with a PSD of (10^-6
* PSI0). The plot1 factor determines if the user requests
for the road profile "z" to be plotted, (i.e. plot1=1).
%The output road profile is put into the 1-D vector z with.
Ns denotes the sampling rate (points per meter).
%The theory behind this code is explained by Georg Rill,
Road Vehicle Dynamics: Fundamentals and Modeling,
%-------------------------------------------------------
%Witten By Farhang Jalilian, University of Victoria.
%Copyright Farhang Jalilian Nov 2013.
%-------------------------------------------------------
function [z,Ns,L1,L2]=genprofile(PSI0,plot1,L)
L1=0;                              %Start length of road
profile (m)
L2=L1+L;                          %End length of road profile
(m)
PSI0=PSI0*10^-6;                  %PSD @ wavenumber(Omega)=1
rad/m
omega1=.01;                        %Low cut-off wavenumber for
PSD
omega2=100;                        %High cut-off wavenumber
for PSD
delta=omega1;                      %Step size for PSD
N=((omega2-omega1)/delta)+2;       %Number of points in PSD
plot
omega=linspace(omega1,omega2,N);%PSD plot wavenumber range
psi=zeros(1,N);                    %Initialize PSD
Ns=100;                            % Number of samples in one
meter of road profile
s=L1:1/Ns:(L2-1/Ns);               %Road profile range
z=zeros(1,Ns*L2);                  %Initialize road
undulations
a=zeros(1,N);                      %Initialize amplitude
coefficients
phi=rand(1,N)*2*pi;                %Random angles
W=2;                               %waviness;
psi(1:N)=PSI0*(omega(1:N).^(-W));%Calculate PSD
a(1:N)=(2*psi(1:N)*(delta)).^(1/2);%Calculate A(i),
Waviness = 2
for i=1:Ns*L2
```

```
    for j=1:N
        z(i)=(a(j)*sin((omega(j)*s(i))-phi(j)))+z(i);
    end
end
z(1:Ns*L2)=z(1:Ns*L2)-z(1);% fix Z(i) initial conditions to
zero
if plot1==1
    figure
    subplot(2,1,1);
    loglog(omega,psi)
    title('PSD of road elevations(undulations) profile');
    xlabel('wavenumber (rad/m)');
    ylabel('PSD m^2/(rad/m)');
    subplot(2,1,2);
    plot(s,z*100);
    title('Road elevations profile');
    xlabel('Road longitudinal axis(m)');
    ylabel('Road vertical undulations(cm)');
    set(gcf, 'Color', 'w');
    export_fig roadrealiz.jpg -m2
end
```